Supplementary Information (SI) for Chemical Science.

Supporting Information

2D-to-3D Transformations of a Covalent Organic Framework via Post-synthetic Crosslinking

Garrison Bauer[a] and Mercedes K. Taylor*[a]

[a]Department of Chemistry and Biochemistry, University of Maryland, College Park, MD 20742, United States

*E-mail: mkt@umd.edu

Table of Contents

Materials: Anhydrous THF was obtained from an Inert solvent purification system. All other chemicals and solvents were purchased from chemical suppliers and were used without further purification.

Nuclear Magnetic Resonance (NMR): Solution-state ^{1}H NMR and ^{13}C NMR spectra were collected on a Bruker AV NEO 400 MHz (NMR400). Chemical shifts are reported in parts per million (ppm) and are referenced to the solvent signal. Solid-state ^{13}C and ^{15}N cross-polarization magic-angle spinning (CPMAS) NMR spectra of COFs were collected on a Bruker Advance NEO solid-state 500m MHz NMR spectrometer with a double resonance H/F-X probe. Carbon-13 chemical shifts concerning TMS by setting $\delta(^{13}C) = 0$ ppm and nitrogen-15 chemical shifts concerning α-glycine by setting $\delta(^{15}N) = 33.4$ ppm. All samples were packed in a 3.2-mm outer diameter zirconia rotor with Kel-F endcap spinning at 14k Hz (^{13}C). The proton-carbon matched cross polarization ramp was at 50 kHz with a 2-ms contact time. The proton dipolar decoupling was achieved during acquisition by applying continuous wave spinal64 on the ^{1}H channel. The $\pi/2$ pulse length was 2.5 μs for ^{1}H, and the recycle delay was 4 s.

Fourier-Transform Infrared (FTIR) Spectroscopy: FTIR was collected on Thermo Nicolet Nexus 670 FTIR ESP with an ATR probe. Data was acquired with solid samples using air from the room as a blank.

Powder X-Ray Diffraction (PXRD): PXRD was carried out with Bruker D8 Advanced diffractometer equipped with a LynxEye detector, X-rays from a Cu Kα radiation ($\lambda = 1.5406$ Å, 40 kV and 40 mA). All PXRD patterns were collected on a scatterless sample holder, starting at a θ-angle of 2.5° to 30° the with a 0.05° step size under ambient conditions.

Gas Sorption Isotherms: Isotherms were measured using a volumetric method on a Micromeritics ASAP 2020 instrument. An empty analysis tube was capped under air at room temperature and weighed. Approximately 100 mg of the sample was weighed in air and transferred to the analysis tube, which was capped under air. The analysis tube was attached to the degassing port of the ASAP 2020 and heated to 100 °C under vacuum overnight. After activation, the tube was backfilled with N_2 and weighed to obtain the sample mass. The analysis tube was then attached to the analysis port of the ASAP 2020 for the surface area measurement. Warm and cold-free spaces were measured using He. N_2 sorption isotherms at 77 K were measured in liquid N_2. Brunauer-Emmett-Teller (BET) surface areas were calculated from the N_2 isotherms at 77 K using points between P/P0 of 0.005 and 0.3 following the Rouquerol criteria. Pore size distributions were calculated using the NLDFT(SD3), N2-77-Carbon Cyl Pores model while minimizing error of fit and roughness of distribution.

Scanning Electron Microscopy (SEM): SEM was performed on a Hitachi SU-70 FEG instrument. Dry powders were deposited onto carbon tape and coated with gold/palladium.

Thermogravimetric Analysis (TGA): TGA was performed on a TA Instruments Discovery TGA-5500. Samples (3−15 mg) were heated in a platinum pan from room temperature to 1000 °C at a heating rate of 10 °C/min under a flow of nitrogen (25 mL/min).

X-Ray Photoelectron Spectroscopy (XPS): XPS was performed on a Kratos Axis Supra operating in Hybrid mode using Monochromatic Al x-rays. Charge neutralization was used. Binding energies were calibrated using the C 1*s* peak at 284.8 eV.

C/H/N/S Combustion Analysis: Combustion analysis was performed by Galbraith Laboratories, Inc., for

COF-V, COF-S_2C_2, COF-S_2C_3, COF-S_2C_4, and COF-S_1C_3 according to the following procedure. Samples, standards, and blanks were prepared in tin capsules and crimped. Blanks and conditioners were run to evaluate system suitability. The instrument was calibrated using known standards. Samples were then analyzed with bracketing QC standards run at least every ten samples. Samples were burned in a PerkinElmer 2400 Series II CHNS/O Analyzer in pure oxygen at 920-980°C under static conditions to produce combustion products of CO_2, H_2O, N_2, and SO_2. The results were then calculated based on the amount of carbon, hydrogen, and nitrogen detected, accounting for the sample mass used.

Synthesis of 2,5-dibromoterephthalaldehyde[1]

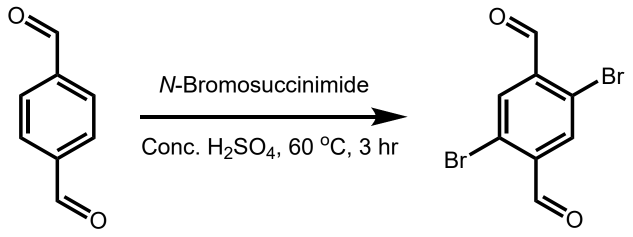

Terephthalaldehyde (10.01 g, 74.60 mmol, 1.0 eq.) was added to concentrated sulfuric acid (101 mL) and heated to 60 °C until complete dissolution. *N*-Bromosuccinimde (28.71 g, 161.3 mmol, 2.2 eq.) was added portion-wise over 15 mins, and the reaction mixture was stirred for 3 hr. The solution was cooled to room temperature and poured over ice, producing a slurry. The precipitate was collected via vacuum filtration and dissolved in dichloromethane. The precipitate was then washed with saturated sodium bicarbonate and brine and dried over anhydrous magnesium sulfate. The solvent was removed via rotary evaporation and recrystallized in ethyl acetate to yield 2,5-dibromoterephthalaldehyde (15.02 g, 69% yield) as pale-yellow crystals. ^{1}H NMR (400 MHz, $CDCl_3$) δ = 10.34 (s, 2H), 8.156 (s, 2H).

Synthesis of 2,5-divinylterephthalaldehyde (DVA)[2,3]

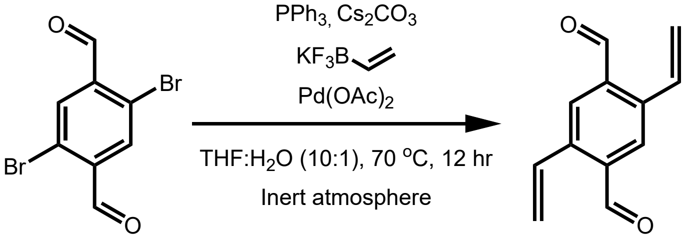

2,5-Dibromoterephthalaldehyde (12.01 g, 41.12 mmol, 1.0 eq.), potassium vinyltrifluoroborate (12.77 g, 95.31 mmol, 2.3 eq.), cesium carbonate (67.13 g, 206.0 mmol, 5.0 eq.), triphenylphosphine (1.097 g, 4.186 mmol, 0.1 eq.), and palladium acetate (0.4698 g, 2.093 mmol, 0.05 eq.) were dissolved in tetrahydrofuran (300 mL) and deionized water (30 mL) under flowing argon. The solution was heated to 70 °C under an inert atmosphere for 12 hr. After the completion of the reaction, sodium diethyldithiocarbamate trihydrate (1.037 g, 4.605 mmol, 2.2 eq.) and 20 mL of DI water were added and stirred for 1 hr. The reaction mixture was further diluted with deionized water and filtered through Celite. The filtrate was extracted with ethyl acetate three times, washed with brine, and dried with anhydrous magnesium sulfate. The crude product was purified via flash column chromatography with hexanes:ethyl acetate (5:1) to yield 2,5-divinylterephthalaldehyde (DVA; 4.755 g, 62% yield) as a pale-yellow powder. ^{1}H NMR (400 MHz, DMSO-d_6) δ = 10.34 (s, 2H), 8.18 (s, 2H), 7.66-7.59 (dd, 2H), 5.97 (d, J = 17.4 Hz, 2H), 5.57 (d, J = 11.1 Hz, 2H).

Synthesis of 1,3,5-tris-(4-nitrophenyl)benzene[4]

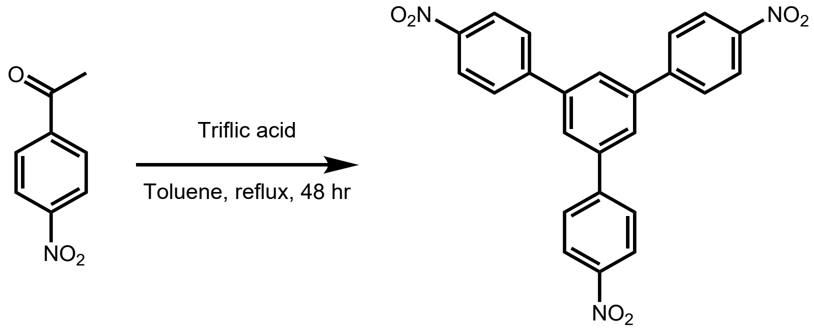

p-Nitroacetophenone (40.03 g, 242.4 mmol, 1.0 eq.), trifluoromethanesulfonic acid (4 mL, 45.4 mmol, 0.19 eq.), and toluene (162 mL) were added to a flask with a Dean-Stark apparatus and a reflux condenser attached. The resulting solution was refluxed for 48 hr. After the reaction flask was cooled, the solution was filtered and washed with acetone to yield a black solid. The black solid underwent Soxhlet extraction with DMF for 72 hr to yield a yellow solid. ^{1}H-NMR was not obtained for the product as it is insoluble in common solvents.

Synthesis of 1,3,5-tris-(4-aminophenyl)benzene (TAPB)[4]

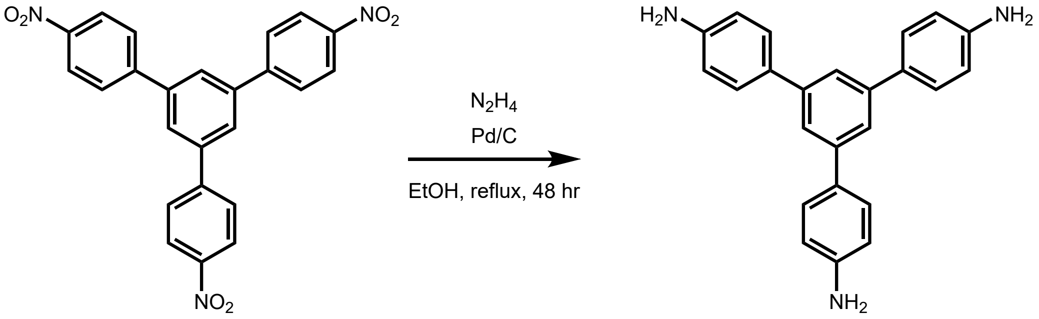

1,3,5-Tris-(4-nitrophenyl)benzene (15.41 g, 34.92 mmol, 1.0 eq.) and 10% Pd/C (1.489 g, 13.99 mmol, 0.4 eq.) were suspended in ethanol (420 mL) and heated to reflux. Hydrazine monohydrate (150 mL, 3090 mmol, 88 eq.) was added and refluxed for 48 hr. The resulting solution was filtered through Cellite, and the filtrate was concentrated by reduced pressure distillation and filtered to yield 1,3,5-tris-(4-aminophenyl)benzene (TAPB; 10.57 g, 86% yield) as white powder. ^{1}H NMR (400 MHz, DMSO-d_6) δ = 7.49 (s, 3H) 7.47 (d, J = 8.7 Hz, 6H), 6.65 (d, J = 8.4 Hz 6H), 5.21 (s, 6H).

Synthesis of (2,5-divinyl-1,4-phenylene)bis(N-phenylmethanimine) (DVI)

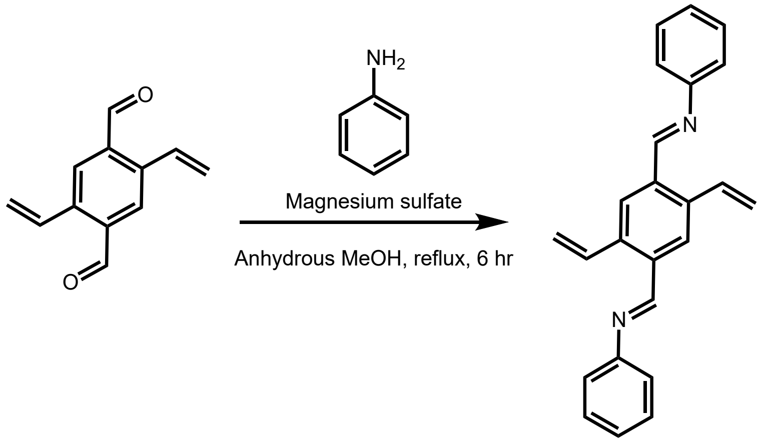

2,5-divinylterephthalaldehyde (93 mg, 0.500 mmol, 1.0 eq.), aniline (91.3 uL, 1.00 mmol, 2.0 eq.), and magnesium sulfate (20 mg) were added to anhydrous methanol (12 mL) and refluxed for 6 hr. The methanol was removed by reduced pressured distillation. The crude solid was dissolved in chloroform and filtered. The solvent was removed by reduced pressure distillation to yield (2,5-divinyl-1,4-phenylene)bis(N-phenylmethanimine) (DVI, 150 mg, 89% yield) as yellow powder. ^{1}H NMR (400 MHz, $CDCl_3$) δ = 8.84 (s, 2H), 8.28 (s, 2H), 7.46 (t, 4H), 7.34-7.29 (dd, 2H), 7.26 (t, 6H), 5.97 (d, *J* = 17.4 Hz, 2H), 5.57 (d, *J* = 11.1 Hz, 2H).

Synthesis of N,N'-((2,5-divinyl-1,4-phenylene)bis(methylene))dianiline (DVAM)

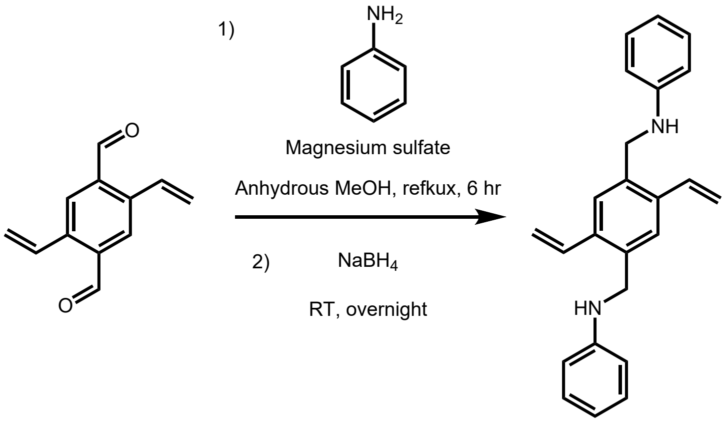

2,5-divinylterephthalaldehyde (93 mg, 0.500 mmol, 1.0 eq.), aniline (91.3 uL, 1.00 mmol, 2.0 eq.), and magnesium sulfate (20 mg) were added to anhydrous methanol (12 mL) and refluxed for 6 hr. After the reaction mixture cooled, sodium borohydride (280 mg, 5 mmol, 5.0 eq.) was added in small portions and stirred overnight. The methanol was removed by reduced pressured distillation. The crude solid was dissolved in chloroform and filtered. The solvent was removed by reduced pressure distillation to yield N,N'-((2,5-divinyl-1,4-phenylene)bis(methylene))dianiline (DVAM; 138 mg g, 81% yield) as white powder. ^{1}H NMR (400 MHz, $CDCl_3$) δ = 7.57 (s, 2H), 7.23 (t, 6H), 7.02-6.95 (dd, 2H), 6.77 (t, 2H), 6.68 (d, *J* = 8.10 Hz, 2H), 5.70 (d, *J* = 17.4 Hz, 2H), 5.32 (d, *J* = 11.1 Hz, 2H).

Synthesis of COF-V[5]

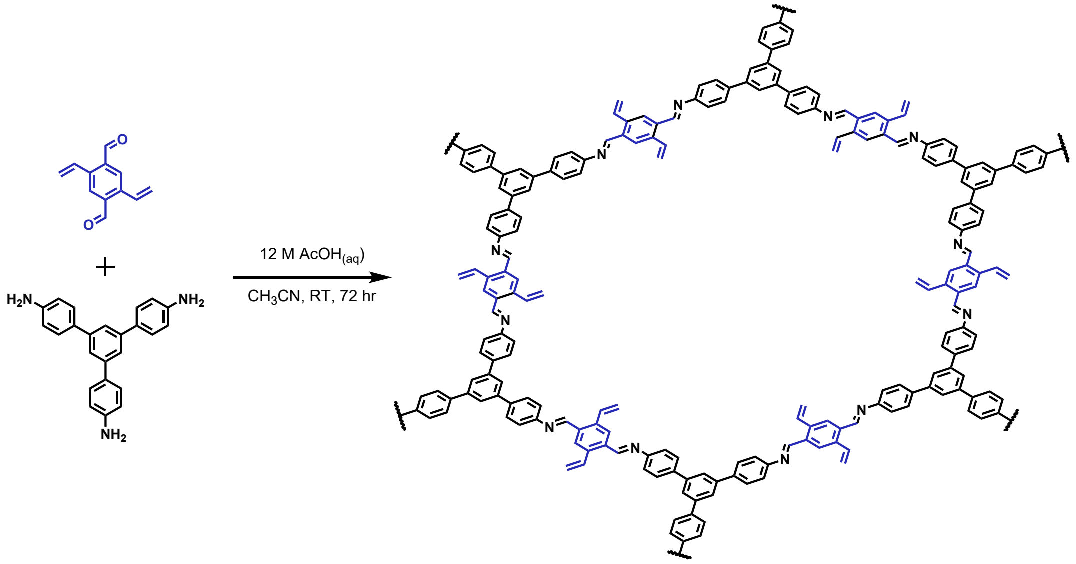

In a 2 L media bottle, 2,5-divinylterephthalaldehyde (0.559 g, 3.00 mmol, 3.0 eq.), 1,3,5-tris-(4-aminophenyl)benzene (0.704 g, 2.00 mmol, 2.0 eq.) and acetonitrile (250 mL) were added and sonicated for 10 min. 12 M acetic acid (20 mL) was added to the solution and shaken vigorously for 2 min. The solution was left undisturbed at room temperature for 72 hr. The resulting yellow suspension was vacuum-filtered and washed via solvent exchange with tetrahydrofuran (400 mL) at 40 °C. The solvent was removed and replaced thrice daily for three days, yielding 1.202 g of bright yellow powder before activation. COF-V was dried under vacuum at 100 °C for 24 hr. The product was characterized by PXRD (Figure 1f), gas sorption isotherm (Figure S8 and S43), ^{13}C CPMAS ssNMR (Figure 1e), ^{15}N CPMAS ssNMR (Figure 2b), FTIR (Figure S6), TGA (Figure S14), and SEM (Figure 1h).

Synthesis of COF-S_2C_2

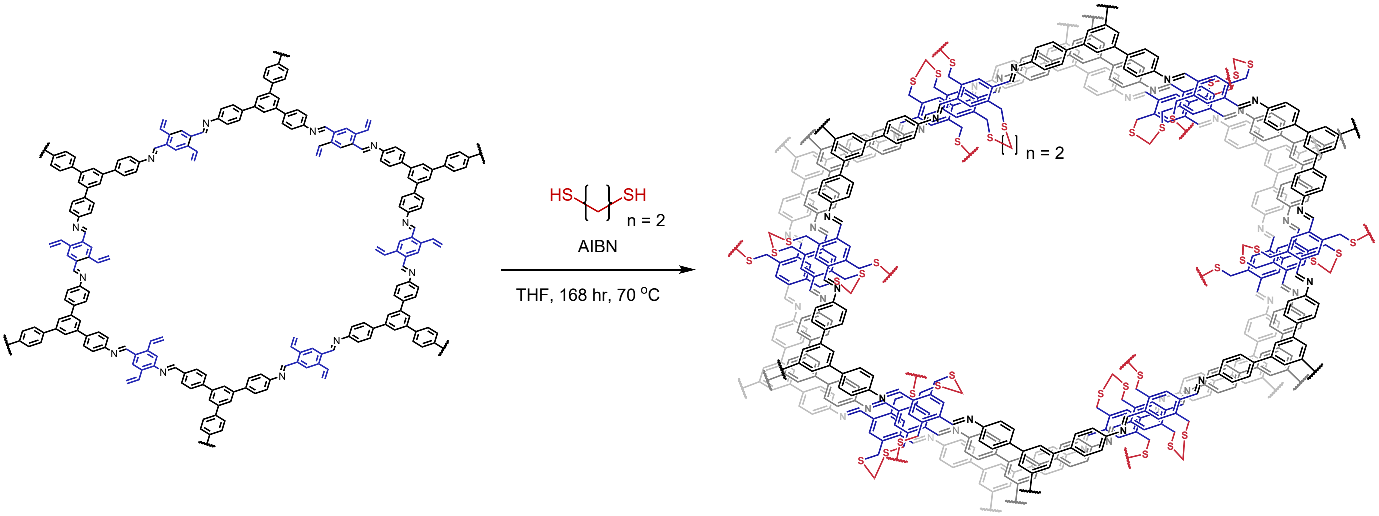

Activated COF-V (100 mg, 0.517 mmol, 1.0 eq.) was suspended in anhydrous tetrahydrofuran (75 mL) under flowing argon. In a separate flask, under an inert atmosphere, 1,2-ethanedithiol (111.3 uL, 0.827 mmol, 1.6 eq.) and azobisisobutyronitrile (AIBN) (4 mg, 0.024 mmol, 0.05 eq.) were dissolved in (15 mL) anhydrous tetrahydrofuran. The reaction flask was heated to 70 °C, and the solution of 1,2-ethanedithiol and AIBN (4 mg, 0.024 mmol, 0.05 eq.) was added dropwise over 12 hr. A solution of the 1,2-ethanedithiol (111.3 uL, 0.827 mmol, 1.6 eq.) and AIBN was added dropwise twice more. After 168 hr, the reaction mixture was vacuum filtered and washed via solvent exchange with tetrahydrofuran (150 mL) then acetone (100 mL) at 40 °C. The solvent was removed and replaced thrice daily for three days, yielding 109 mg of yellow powder. The product was characterized by PXRD (Figure 1f), gas sorption isotherm (Figure S24), ^{13}C CPMAS ssNMR (Figure 1e), FTIR (Figure S9), XPS (Figure S13), TGA (Figure S15), and SEM (Figure 1i).

Synthesis of COF-S_2C_3

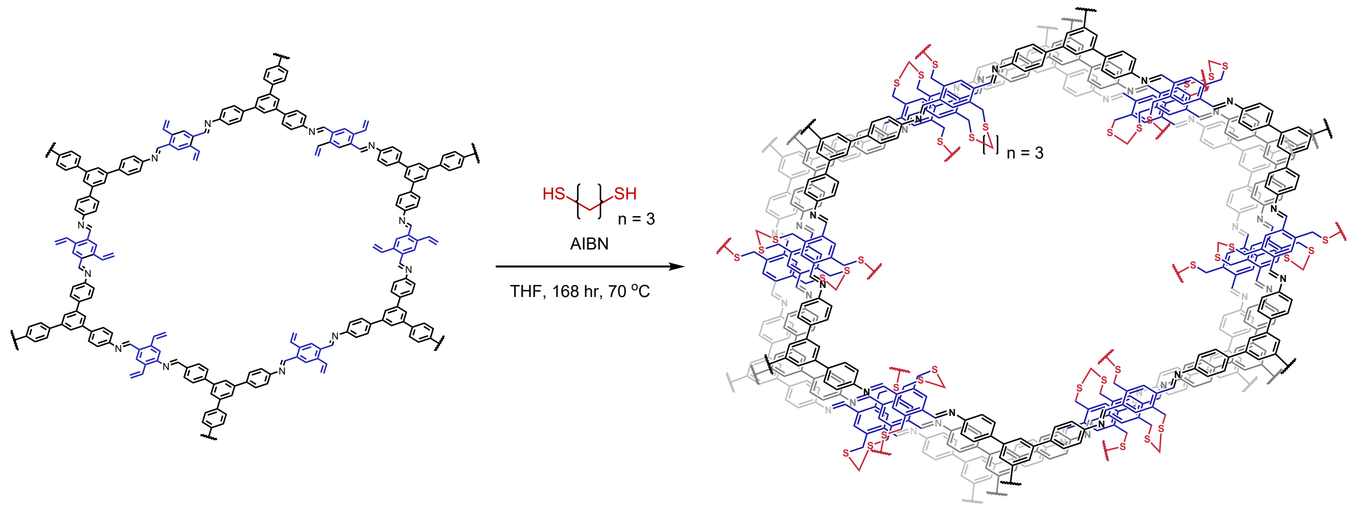

Activated COF-V (100 mg, 0.517 mmol, 1.0 eq.) was suspended in anhydrous tetrahydrofuran (75 mL) under flowing argon. In a separate flask, under an inert atmosphere, 1,3-propanedithiol (82.9 uL, 0.827 mmol, 1.6 eq.) and AIBN (4 mg, 0.024 mmol, 0.05 eq.) were dissolved in anhydrous tetrahydrofuran (15 mL). The reaction flask was heated to 70 °C, and the solution of dithiol crosslinker was added dropwise over 12 hr. A solution of the 1,3-propanedithiol (82.9 uL, 0.827 mmol, 1.6 eq.) and AIBN (4 mg, 0.024 mmol, 0.05 eq.) was added dropwise twice more. After 168 hr, the reaction mixture was vacuum filtered and washed via solvent exchange with tetrahydrofuran (150 mL), then acetone (100 mL) at 40 °C. The solvent was removed and replaced thrice daily for three days, yielding 111 mg of yellow powder. The product was characterized by PXRD (Figure 1f), gas sorption isotherm (Figure S25), ^{13}C CPMAS ssNMR (Figure 1e), FTIR (Figure S10), XPS (Figure S13), TGA (Figure S16), and SEM (Figure 1j).

Synthesis of COF-S_2C_4

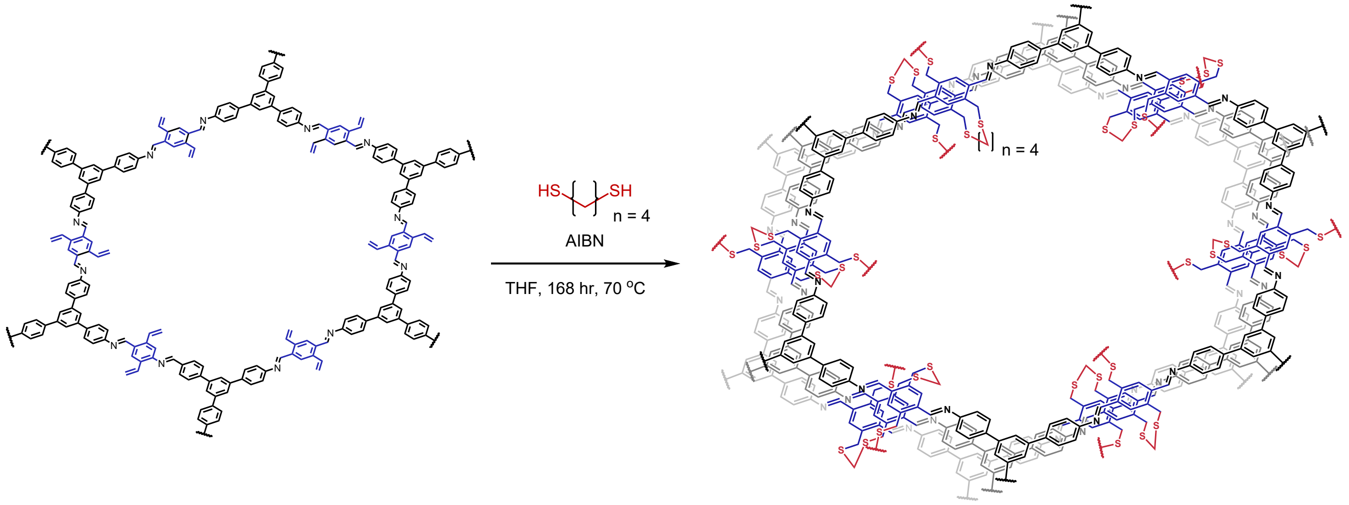

Activated COF-V (100 mg, 0.517 mmol, 1.0 eq.) was suspended in anhydrous tetrahydrofuran (75 mL) under flowing argon. In a separate flask, under an inert atmosphere, 1,4-butanedithiol (97.0 uL, 0.827 mmol, 1.6 eq.) and AIBN AIBN (4 mg, 0.024 mmol, 0.05 eq.) were dissolved in anhydrous tetrahydrofuran (15 mL). The reaction flask was heated to 70 ˚C, and the solution of 1,4-butanedithiol (97.0 uL, 0.827 mmol, 1.6 eq.) and AIBN (4 mg, 0.024 mmol, 0.05 eq.) was added dropwise over 12 hr. A solution of the dithiol crosslinker and AIBN was added dropwise twice more. After 168 hr, the reaction mixture was vacuum filtered and washed via solvent exchange with tetrahydrofuran (150 mL), then acetone (100 mL) at 40 ˚C. The solvent was removed and replaced thrice daily for three days, yielding 115 mg of yellow powder. The product was characterized by PXRD (Figure 1f), gas sorption isotherm (Figure S26), ^{13}C CPMAS ssNMR (Figure 1e), FTIR (Figure S11), XPS (Figure S13), TGA (Figure S17), and SEM (Figure 1k).

Synthesis of COF-S_1C_3[6]

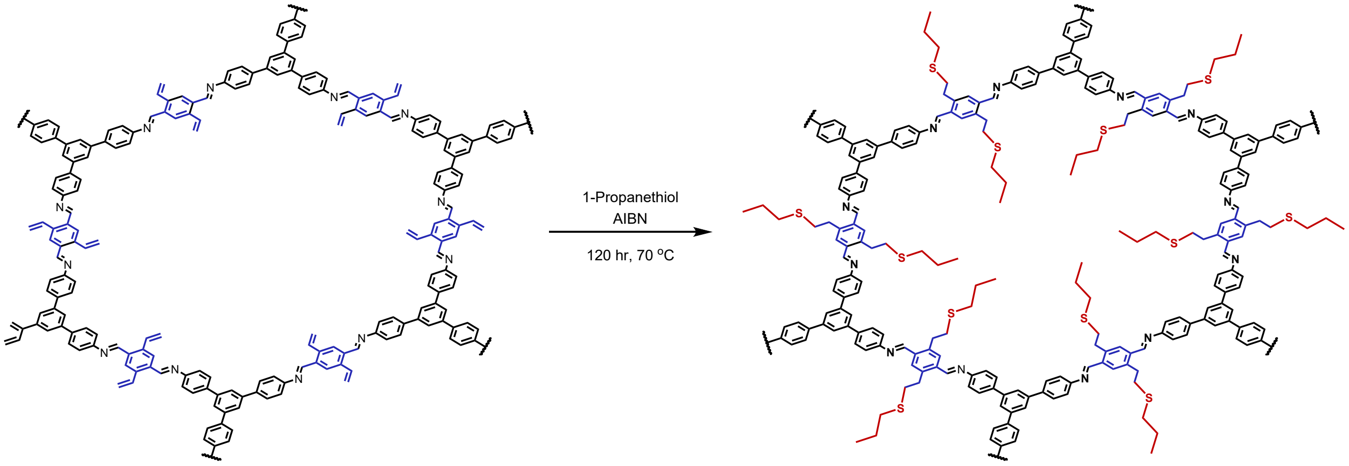

Activated COF-V (150 mg, 0.776 mmol, 1.0 eq.) was suspended in 1-propanethiol (30 mL, 323 mmol, 0.0 eq.), and AIBN (10 mg, 0.06 mmol, 0.08 eq.) was added under flowing argon. The reaction flask was heated to 70 °C for 72 hr. A second portion of AIBN (10 mg, 0.122 mmol, 0.08 eq.) was added, and the reaction was heated for another 48 hr. After 120 hr, the reaction mixture was vacuum filtered and washed via solvent exchange with tetrahydrofuran (150 mL) and acetone (100 mL) at 40 °C. The solvent was removed and replaced thrice daily for three days, yielding 178 mg of yellow powder. The product was characterized by PXRD (Figure 1f), gas sorption isotherm (Figure S27), ^{13}C CPMAS ssNMR (Figure 1e), FTIR (Figure S12), XPS (Figure S13), TGA (Figure S18), and SEM (Figure 1l).

Synthesis of COF-V-R[7]

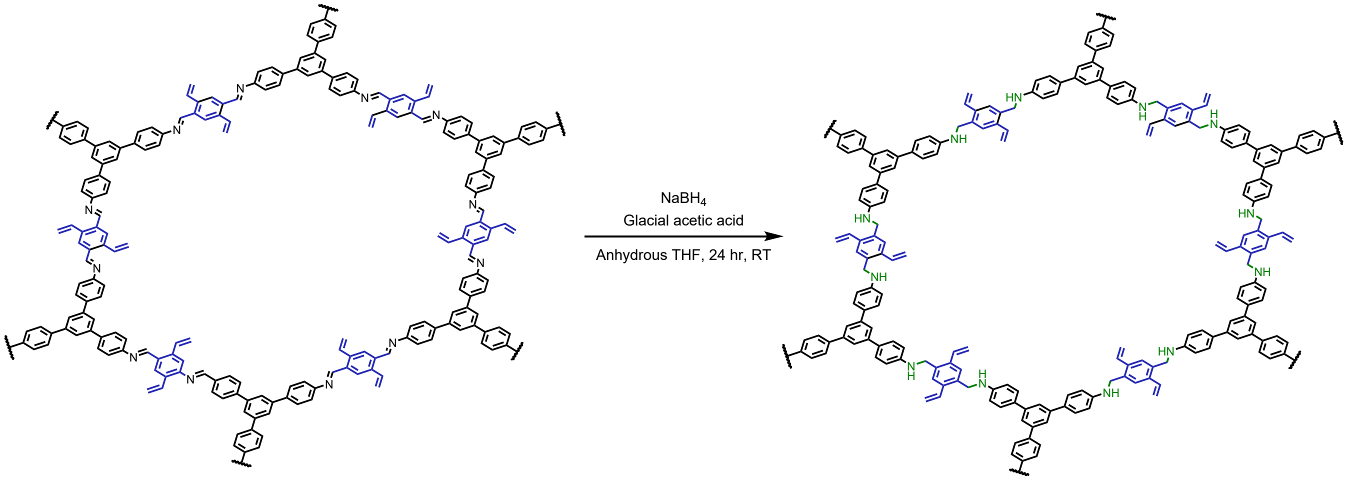

Adapted from a literature procedure, activated COF-V (100 mg, 0.518 mmol, 1.0 eq.) and sodium borohydride (195 mg, 5.18 mmol, 10.0 eq.) were suspended in anhydrous tetrahydrofuran (25 mL) under flowing argon. Glacial acetic acid (44.4 uL, 0.777 mmol, 1.5 eq.) was added, and the reaction mixture was stirred at room temperature for 24hr. The reaction mixture was vacuum filtered and washed via solvent exchange with methanol (150 mL) at 40 °C. The solvent was removed and replaced thrice daily for three days, yielding 116 mg of yellow powder. The product was characterized by PXRD (Figure 2d), gas sorption isotherm (Figure 3a and S37), ^{13}C CPMAS ssNMR (Figure S28), ^{15}N CPMAS ssNMR (Figure 2b), FTIR (Figure 2c), and SEM (Figure 2e).

Synthesis of COF-S$_2$C$_2$-R[7]

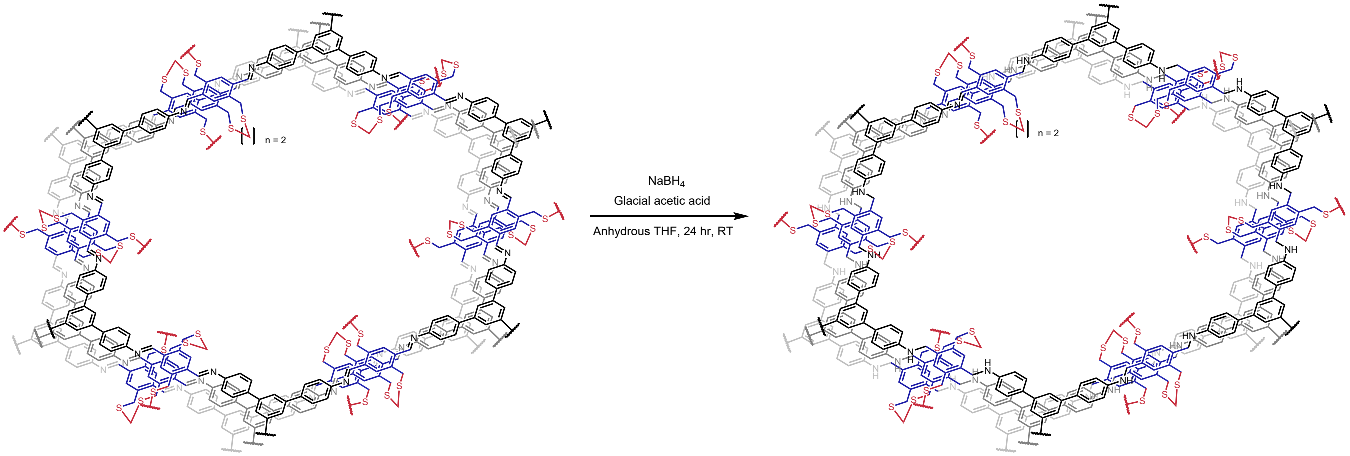

Adapted from a literature procedure, activated COF-S$_2$C$_2$ (100 mg, 0.417 mmol, 1.0 eq.) and sodium borohydride (158 mg, 4.17 mmol, 10.0 eq.) were suspended in anhydrous tetrahydrofuran (20 mL) under flowing argon. Glacial acetic acid (35.7 uL, 0.626 mmol, 1.5 eq.) was added, and the reaction mixture was stirred at room temperature for 24hr. The reaction mixture was vacuum filtered and washed via solvent exchange with methanol (150 mL) at 40 °C. The solvent was removed and replaced thrice daily for three days, yielding 108 mg of yellow powder. The product was characterized by PXRD (Figure 2d), gas sorption isotherm (Figure 3a), ^{13}C CPMAS ssNMR (Figure S29), FTIR (Figure 2c), and SEM (Figure 2f).

Synthesis of COF-S_2C_3-R[7]

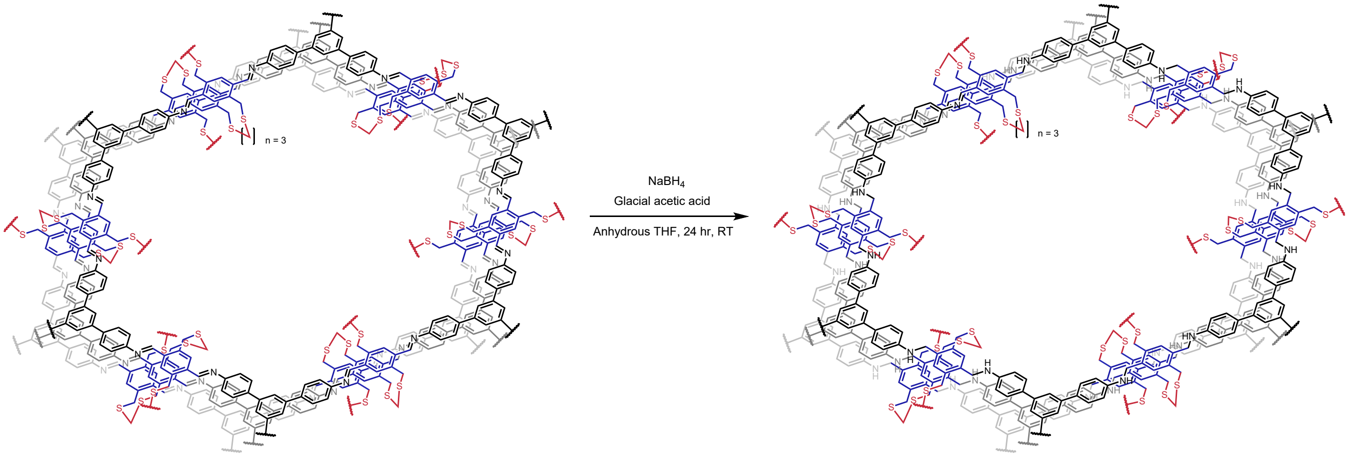

Adapted from a literature procedure, activated COF-S_2C_3 (100 mg, 0.406 mmol, 1.0 eq.) and sodium borohydride (154 mg, 4.06 mmol, 10.0 eq.) were suspended in anhydrous tetrahydrofuran (19 mL) under flowing argon. Glacial acetic acid (34.8 uL, 0.609 mmol, 1.5 eq.) was added, and the reaction mixture was stirred at room temperature for 24hr. The reaction mixture was vacuum filtered and washed via solvent exchange with methanol (150 mL) at 40 °C. The solvent was removed and replaced thrice daily for three days, yielding 105 mg of yellow powder. The product was characterized by PXRD (Figure 2d), gas sorption isotherm (Figure 3a), ^{13}C CPMAS ssNMR (Figure S30), ^{15}N CPMAS ssNMR (Figure 2b), FTIR (Figure 2c), and SEM (Figure 2g).

Synthesis of COF-S_2C_4-R [7]

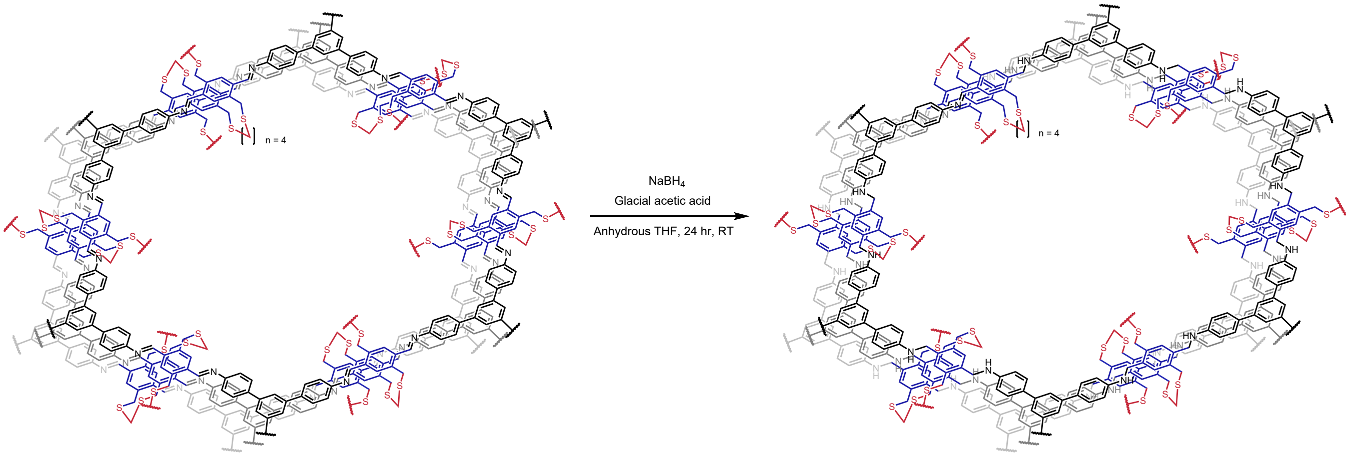

Adapted from a literature procedure, activated COF-S_2C_4 (100 mg, 0.394 mmol, 1.0 eq.) and sodium borohydride (149 mg, 3.94 mmol, 10.0 eq.) were suspended in anhydrous tetrahydrofuran (19 mL) under flowing argon. Glacial acetic acid (33.8 uL, 0.591 mmol, 1.5 eq.) was added, and the reaction mixture was stirred at room temperature for 24hr. The reaction mixture was vacuum filtered and washed via solvent exchange with methanol (150 mL) at 40 ^{o}C. The solvent was removed and replaced thrice daily for three days, yielding 103 mg of yellow powder. The product was characterized by PXRD (Figure 2d), gas sorption isotherm (Figure 3a), ^{13}C CPMAS ssNMR (Figure S31), FTIR (Figure 2c), and SEM (Figure 2h).

Synthesis of COF- S_1C_3-R [7]

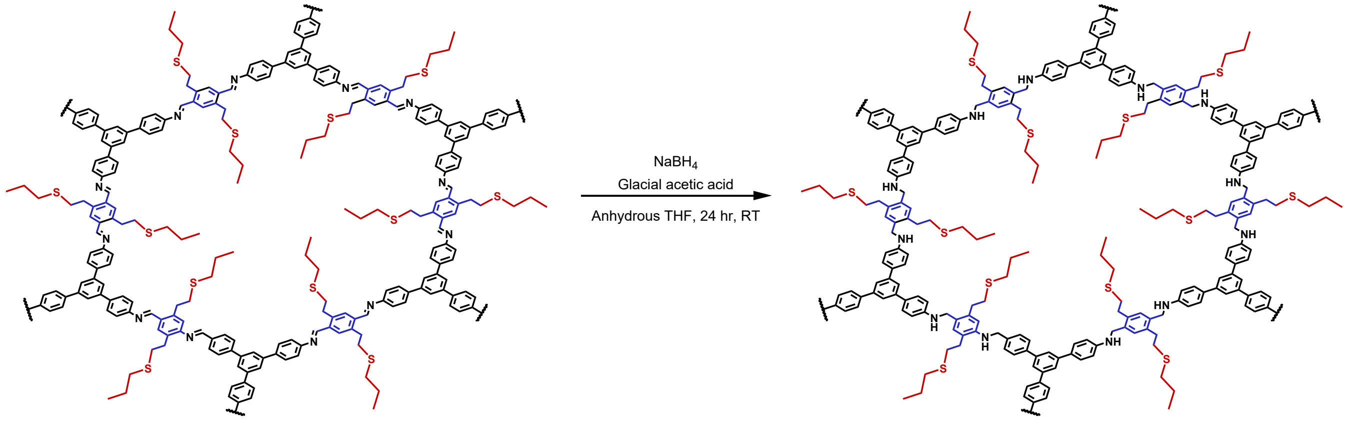

Adapted from a literature procedure, activated COF- S_1C_3 (100 mg, 0.373 mmol, 1.0 eq.) and sodium borohydride (141 mg, 3.73 mmol, 10.0 eq.) were suspended in anhydrous tetrahydrofuran (18 mL) under flowing argon. Glacial acetic acid (32.0 uL, 0.560 mmol, 1.5 eq.) was added, and the reaction mixture was stirred at room temperature for 24hr. The reaction mixture was vacuum filtered and washed via solvent exchange with methanol (150 mL) at 40 ^{o}C. The solvent was removed and replaced thrice daily for three days, yielding 108 mg of yellow powder. The product was characterized by PXRD (Figure 2d), gas sorption isotherm (Figure 3a), ^{13}C CPMAS ssNMR (Figure S32), FTIR (Figure 2c), and SEM (Figure 2i).

Synthesis of COF-S$_2$C$_3$-Ac[7]

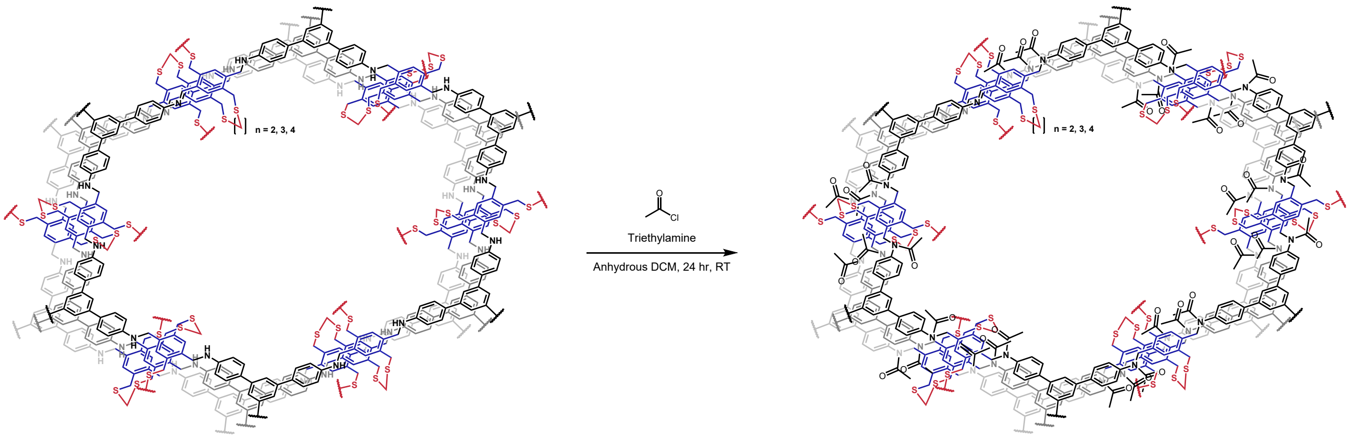

Adapted from a literature procedure, activated COF-S$_2$C$_3$-R (50 mg, 0.201 mmol, 1.0 eq.) was suspended in anhydrous dichloromethane (10 mL) under flowing argon. Triethylamine (421 uL, 3.02 mmol, 15.0 eq.) was added, and the reaction mixture was cooled to 0 ^{o}C. After 10 minutes, acetyl chloride (600 uL, 2.03 mmol, 10.1 eq.) was added and warmed to room temperature for 24hr. The reaction mixture was vacuum filtered and washed via solvent exchange with dichloromethane (50 mL), acetone (100 mL), water (100 mL), and ethanol (100 mL). Each solvent was removed and replaced thrice daily for one day, yielding 53 mg of yellow powder. The product was characterized by PXRD (Figure S40), gas sorption isotherm (Figure S42 and S44), ^{13}C CPMAS ssNMR (Figure 4a), FTIR (Figure S39), ^{15}N CPMAS ssNMR (Figure 4b), and SEM (Figure 41).

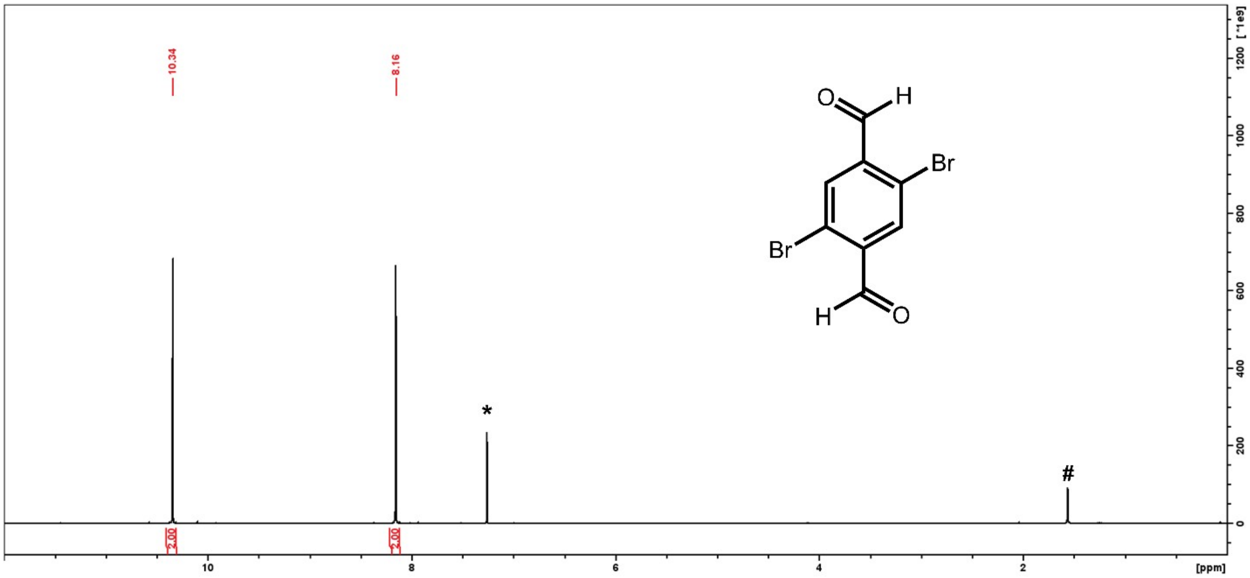

Figure S1. ^{1}H NMR spectrum (400 MHz, $CDCl_3$) of 2,5-dibromoterephthalaldehyde (* = $CDCl_3$ and # = water).

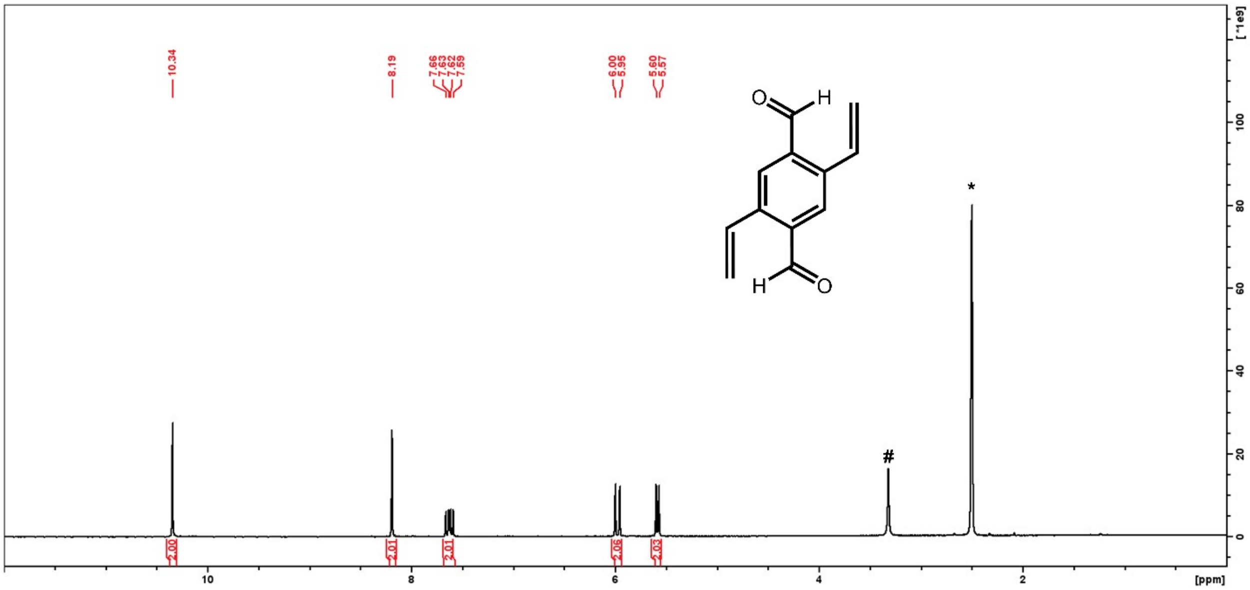

Figure S2. ^{1}H NMR spectrum (400 MHz, DMSO-d_6) of divinylterephthalaldehyde (* = DMSO-d_6 and # = water).

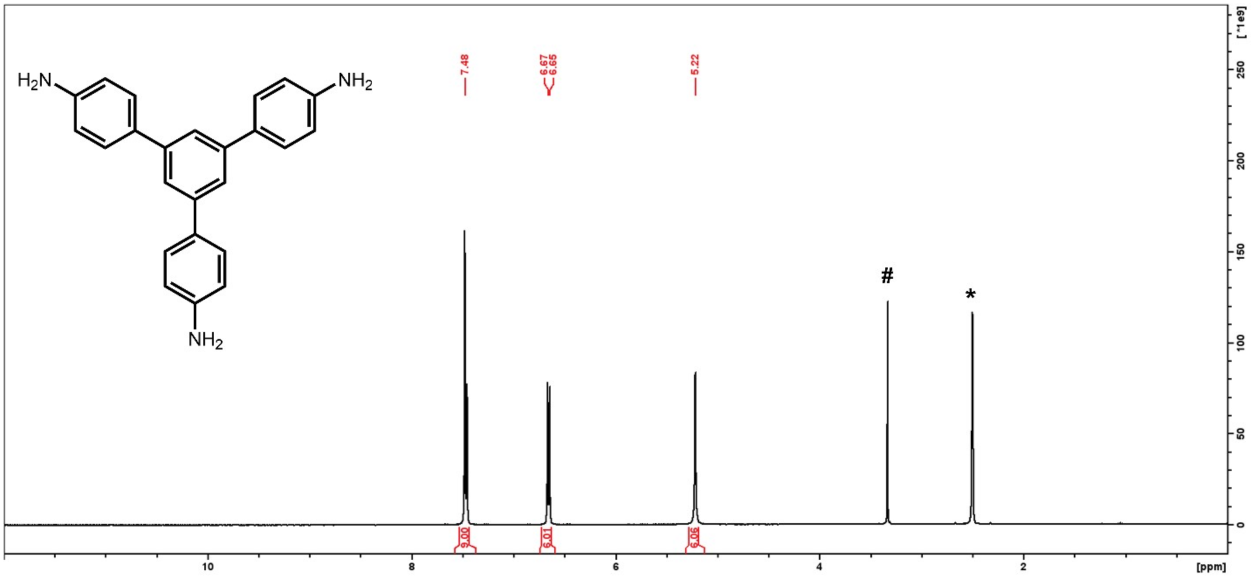

Figure S3. ^{1}H NMR spectrum (400 MHz, DMSO-d_6) of 1,3,5-tris-(4-aminophenyl)benzene (* = DMSO-d_6 and # = water).

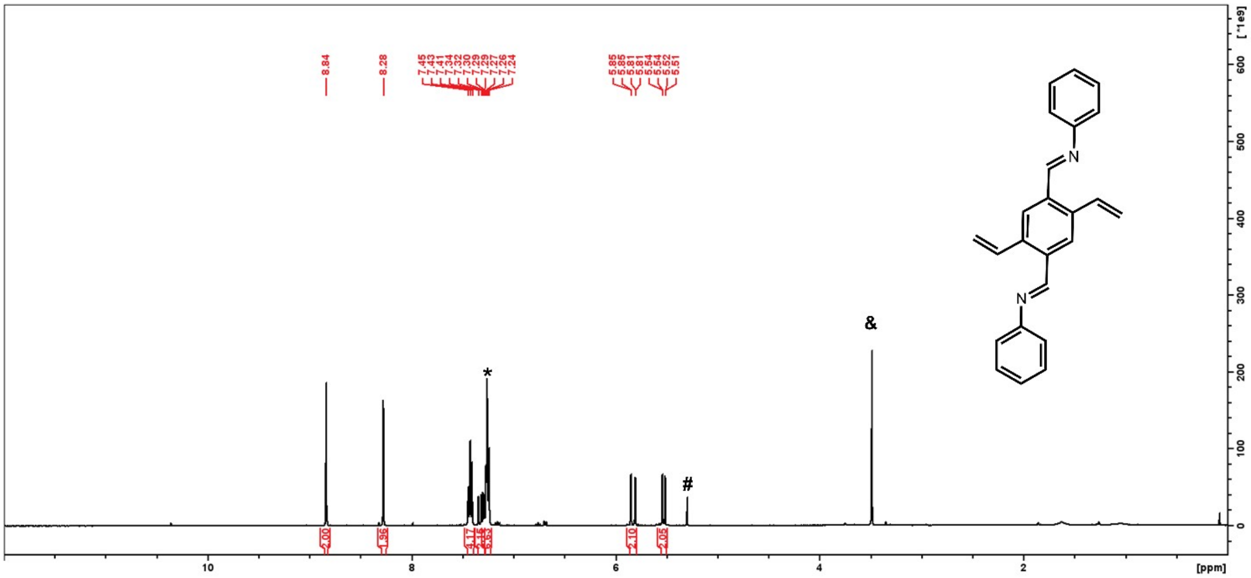

Figure S4. ^{1}H NMR spectrum (400 MHz, $CDCl_3$) of 2,5-divinyl-1,4-phenylene)bis(N-phenylmethanimine (DVI; * = $CDCl_3$, # = dichloromethane, and & = methanol).

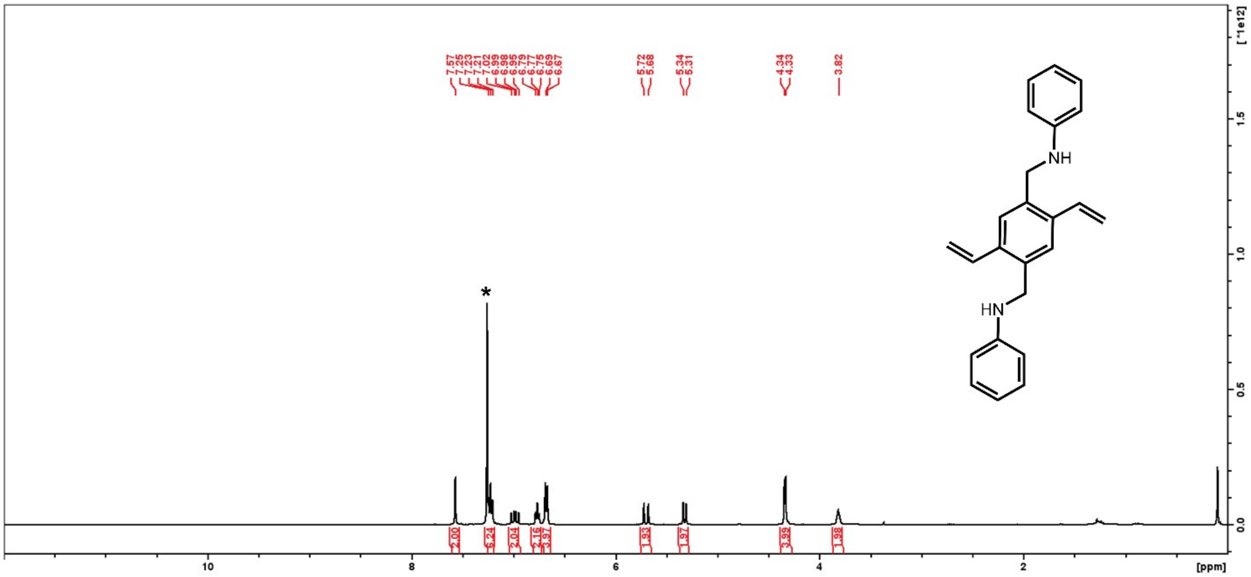

Figure S5. ^{1}H NMR spectrum (400 MHz, $CDCl_3$) of *N*,*N'*-(2,5-divinyl-1,4-phenylene)bis(methylene)dianiline (DVAM; * = $CDCl_3$).

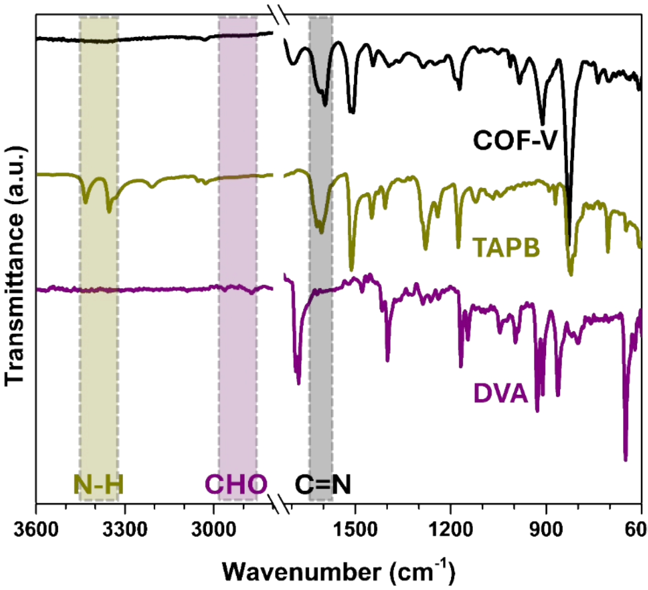

Figure S6. Comparison of FTIR spectra of COF-V (black), TAPB (gold), and DVA (purple).

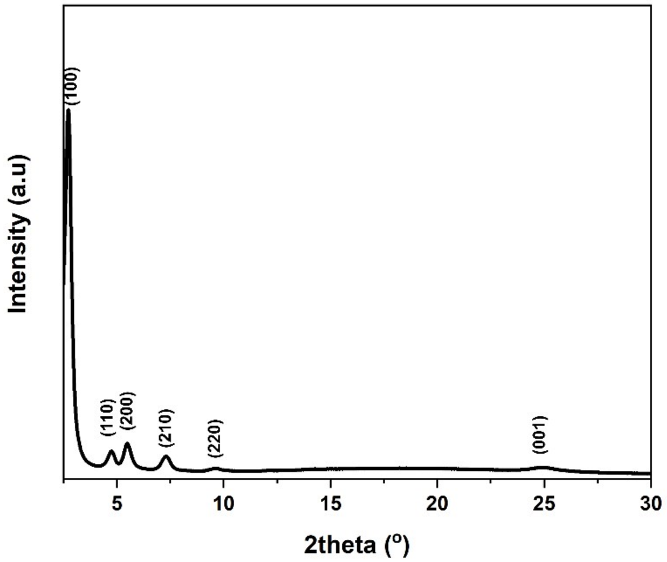

Figure S7. PXRD pattern of COF-V.[6]

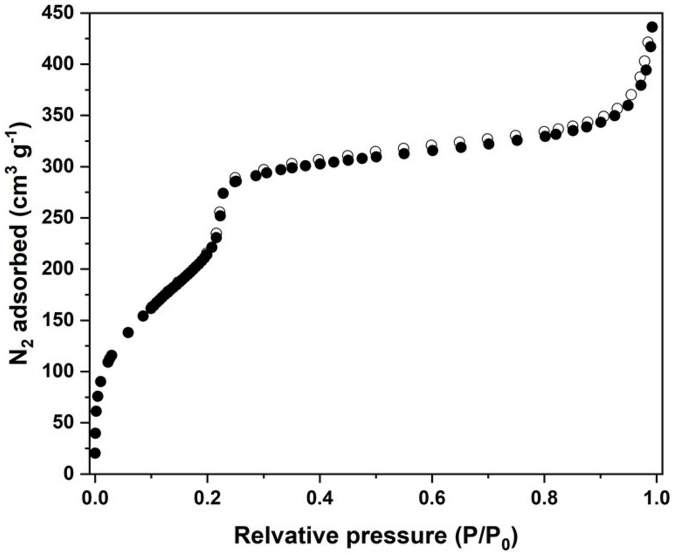

Figure S8. N_2 sorption isotherm of COF-V at 77 K (BET surface area = 930 m^2/g, literature BET surface area = 1052 m^2/g).[5]

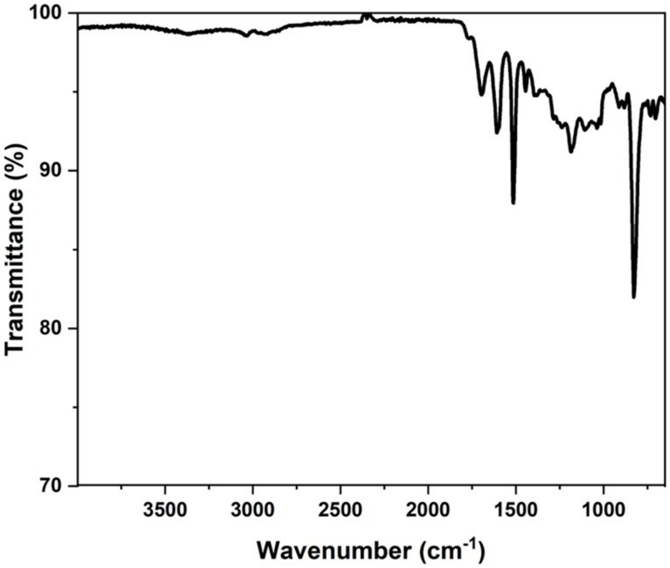

Figure S9. FTIR spectrum of COF-S_2C_2.

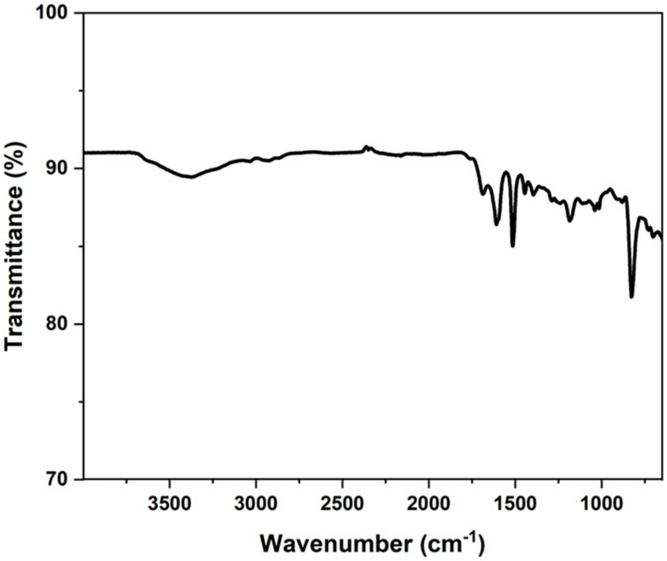

Figure S10. FTIR spectrum of COF-S_2C_3.

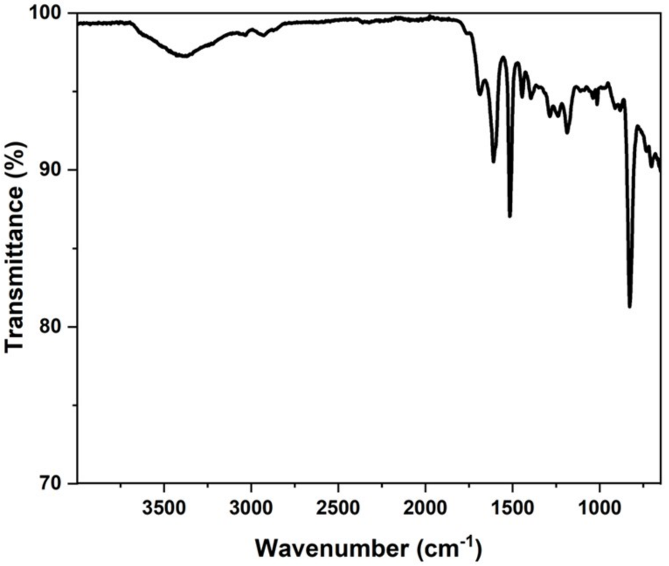

Figure S11. FTIR spectrum of COF-S_2C_4.

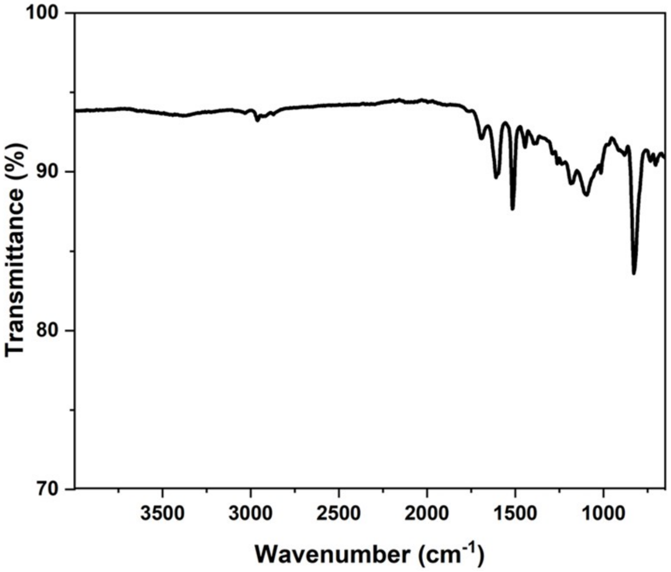

Figure S12. FTIR spectrum of COF-S_1C_3.

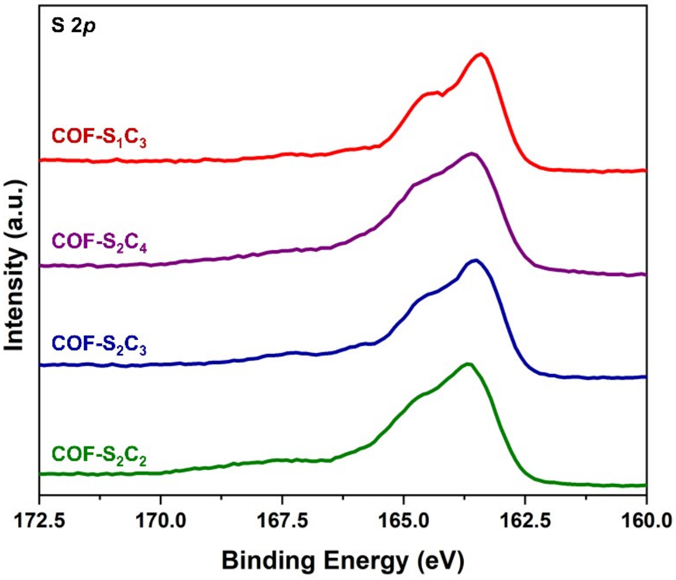

Figure S13. Comparison of S 2*p* XPS spectrum for COF-S_2C_2 (green), COF-S_2C_3 (blue), COF-S_2C_4 (purple), and COF-S_1C_3 (red).

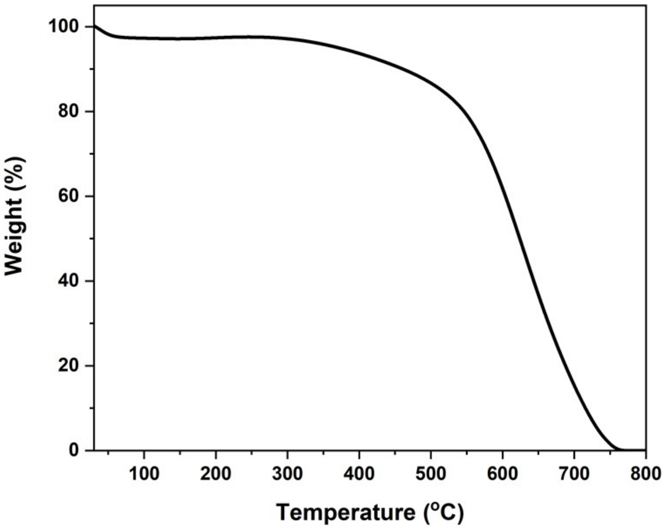

Figure S14. TGA of COF-V.

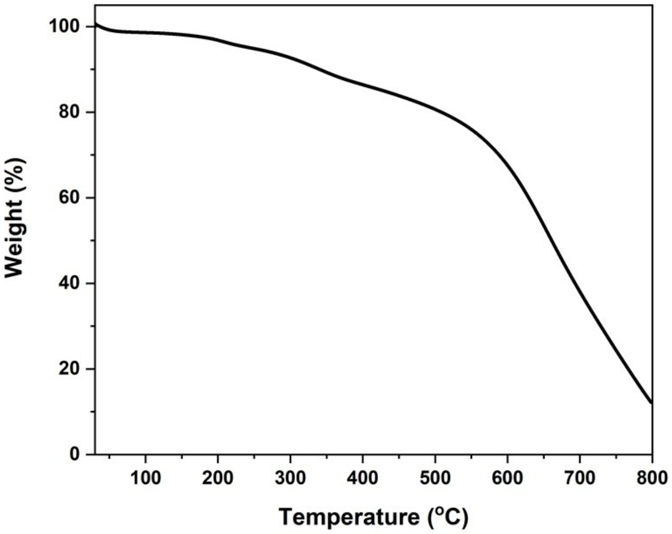

Figure S15. TGA of COF-S_2C_2.

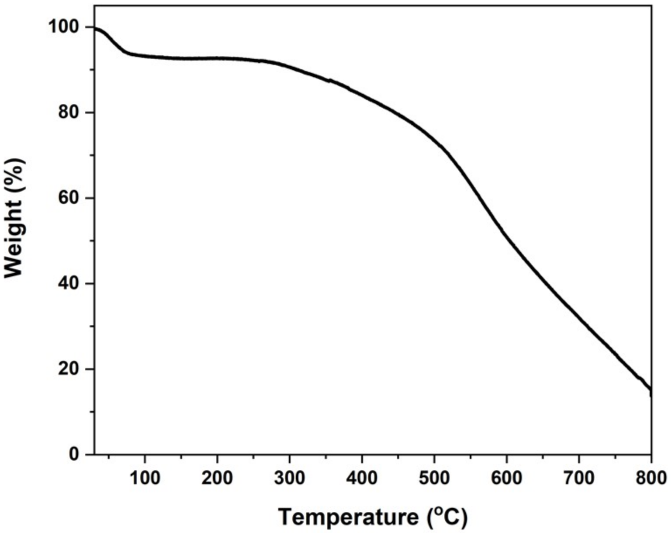

Figure S16. TGA of COF-S_2C_3.

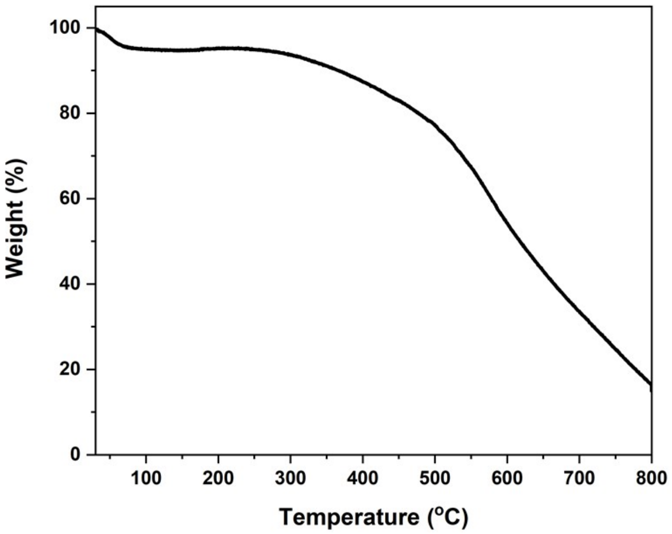

Figure S17. TGA of COF-S_2C_4.

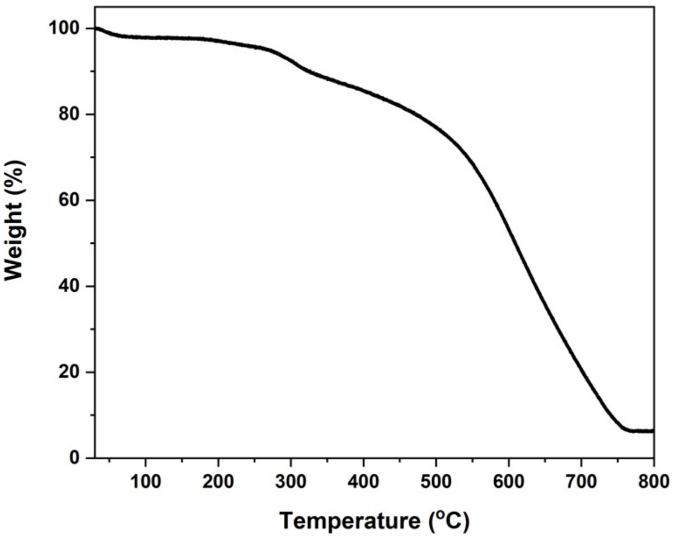

Figure S18. TGA of COF-S_1C_3.

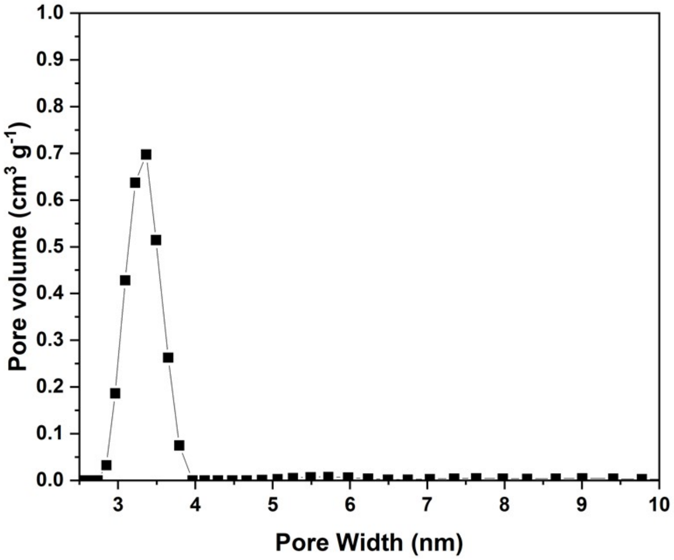

Figure S19. Calculated pore size distribution of COF-V.

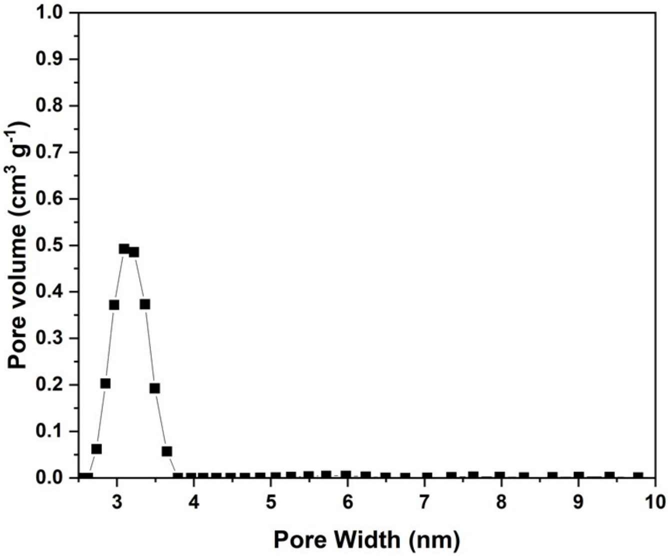

Figure S20. Calculated pore size distribution of COF-S_2C_2.

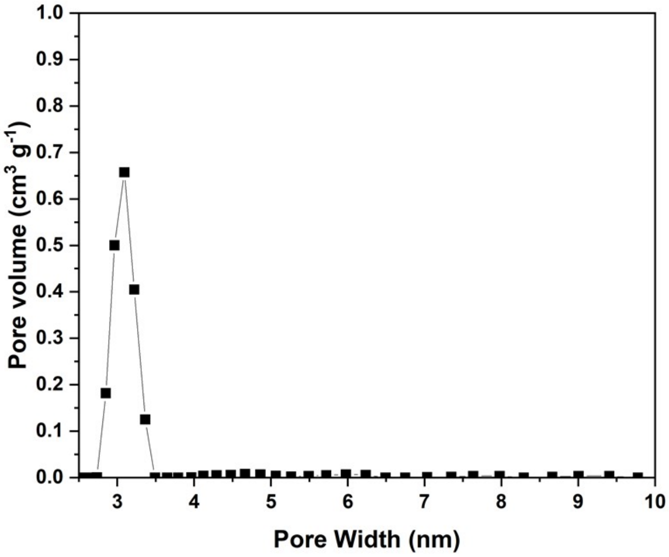

Figure S21. Calculated pore size distribution of COF-S_2C_3.

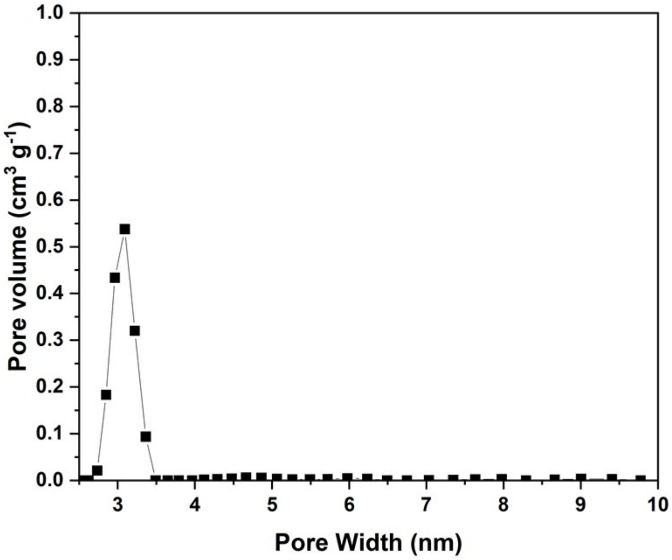

Figure S22. Calculated pore size distribution of COF-S_2C_4.

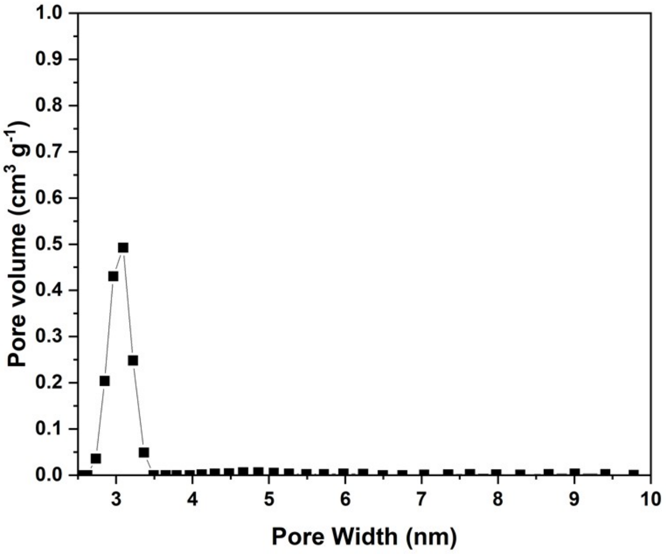

Figure S23. Calculated pore size distribution of COF-S_1C_3.

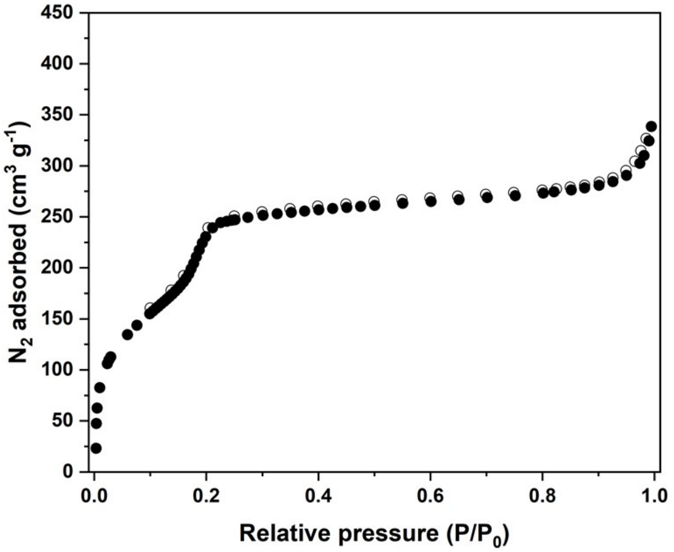

Figure S24. N_2 sorption isotherm of COF-S_2C_2 at 77 K.

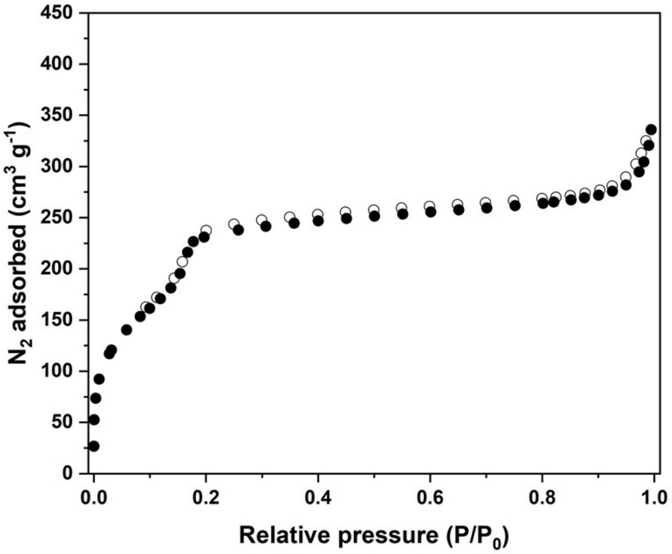

Figure S25. N_2 sorption isotherm of COF-S_2C_3 at 77 K.

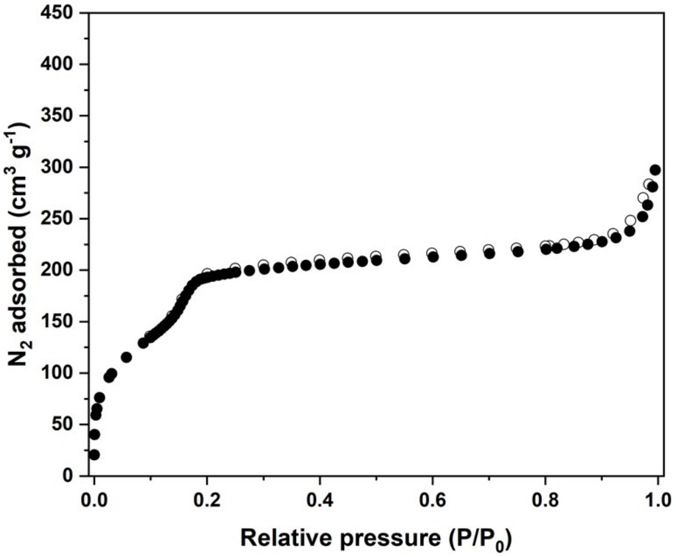

Figure S26. N_2 sorption isotherm of COF-S_2C_4 at 77 K.

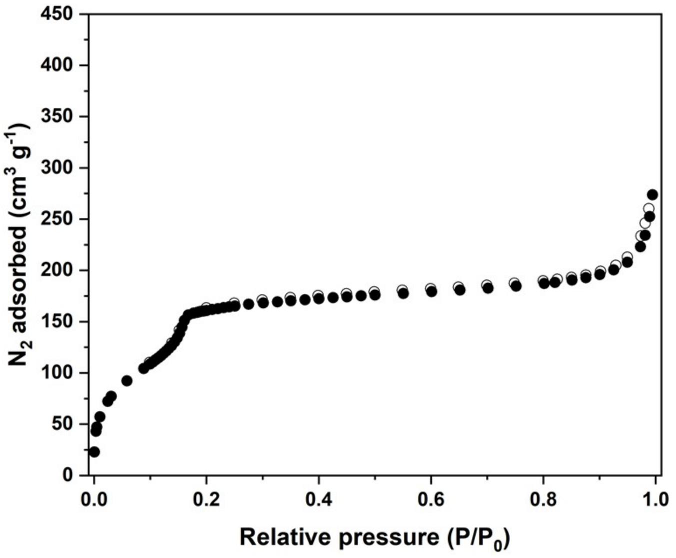

Figure S27. N_2 sorption isotherm of COF-S_1C_3 at 77 K.

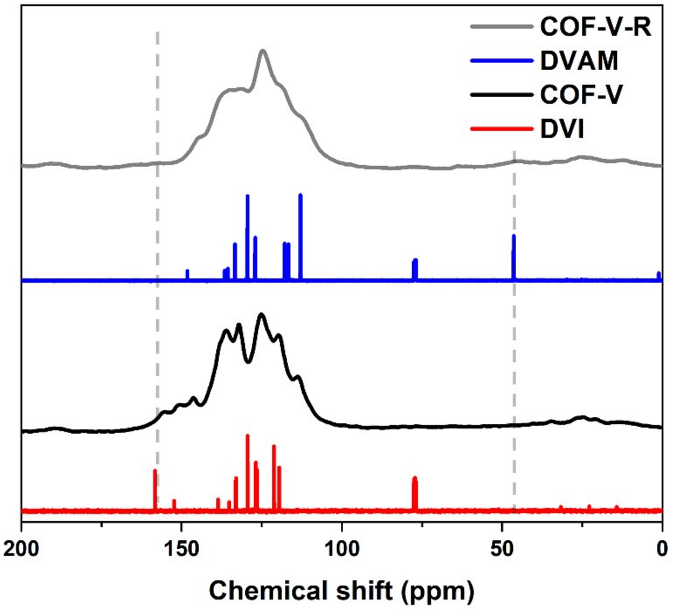

Figure S28. Comparison of ^{13}C NMR spectrum (400 MHz, $CDCl_3$) of 2,5-divinyl-1,4-phenylene)bis(N-phenylmethanimine (DVI; red) and 2,5-divinyl-1,4-phenylene)bis(methylene))dianiline (DVAM; blue) and ^{13}C CPMAS ssNMR spectra of COF-V (black) and COF-V-R (grey).

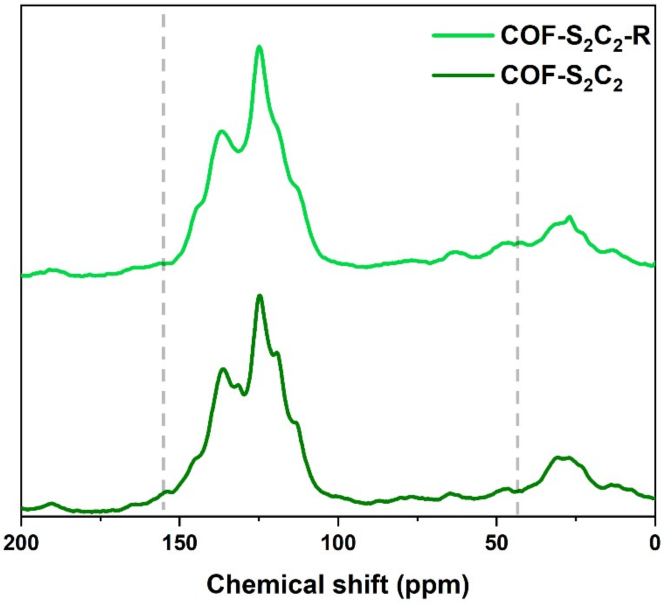

Figure S29. Comparison of ^{13}C CPMAS ssNMR spectra of COF-S_2C_2 (dark green) and COF-S_2C_2-R (light green).

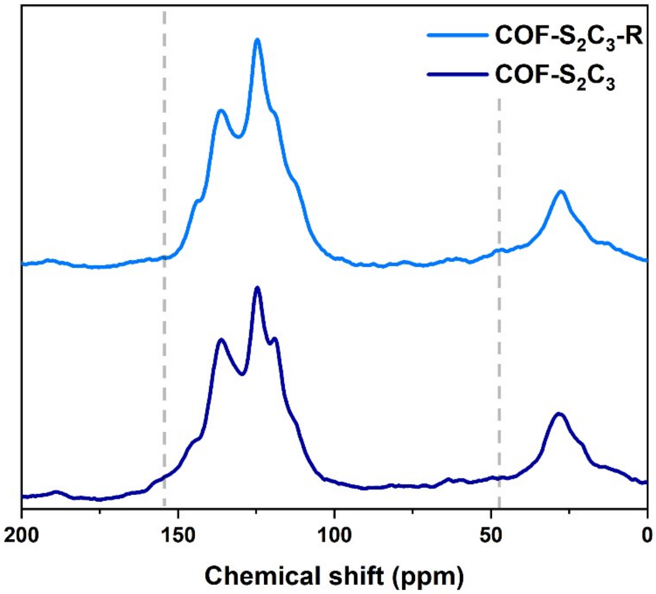

Figure S30. Comparison of ^{13}C CPMAS ssNMR spectra of COF-S_2C_3 (dark blue) and COF-S_2C_3-R (light blue).

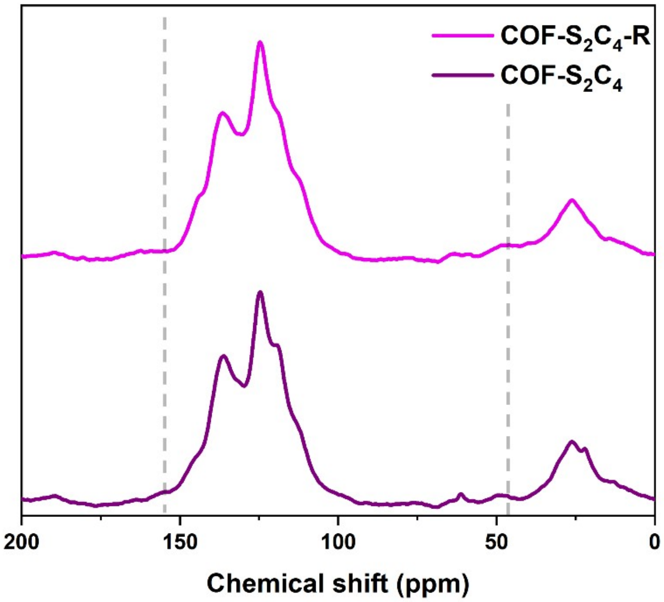

Figure S31. Comparison of ^{13}C CPMAS ssNMR spectra of COF-S_2C_4 (purple) and COF-S_2C_4-R (pink).

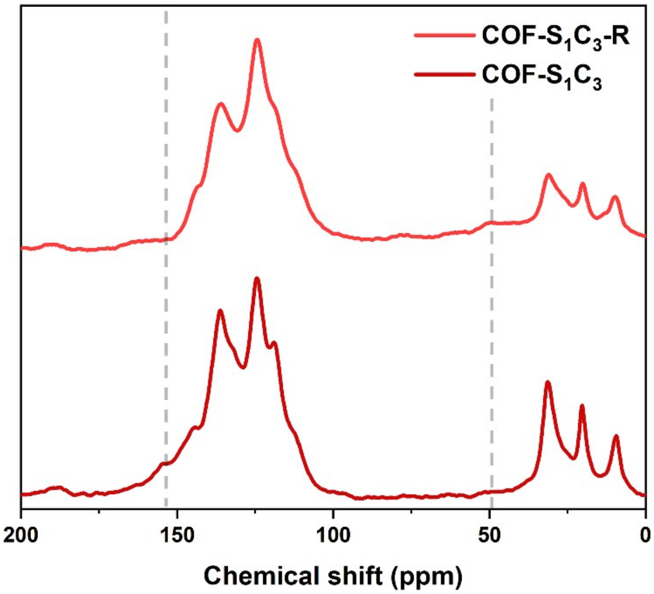

Figure S32. Comparison of ^{13}C CPMAS ssNMR spectra of COF-S_1C_3 (dark red) and COF-S_1C_3-R (red).

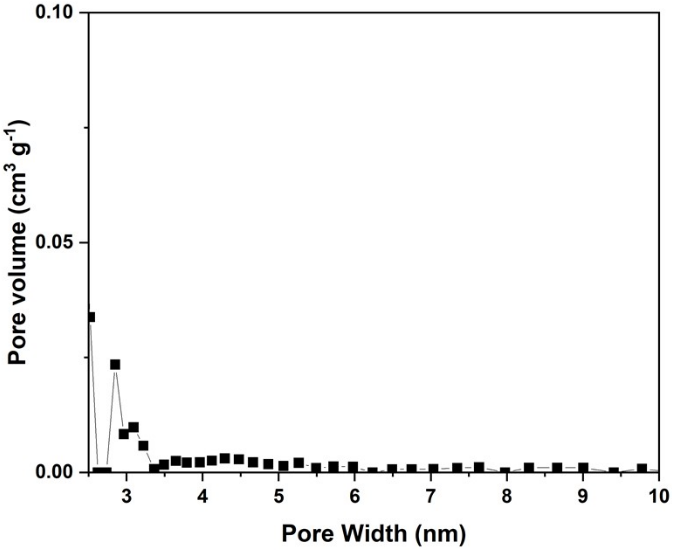

Figure S33. Calculated pore size distribution of COF-V-R.

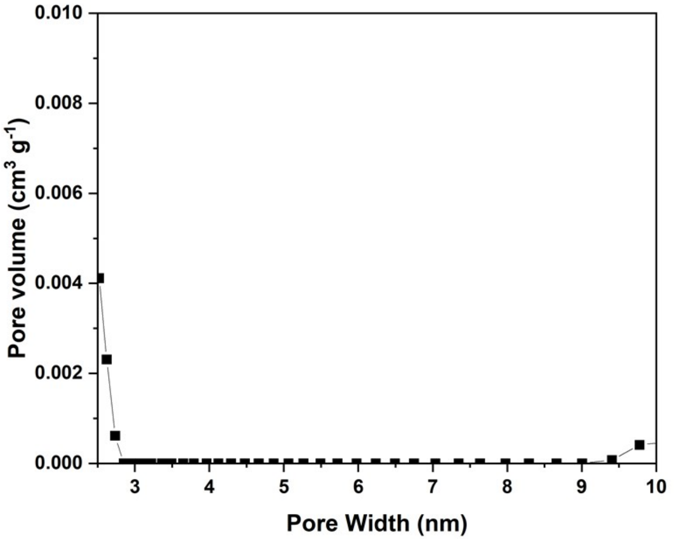

Figure S34. Calculated pore size distribution of COF-S_1C_3-R.

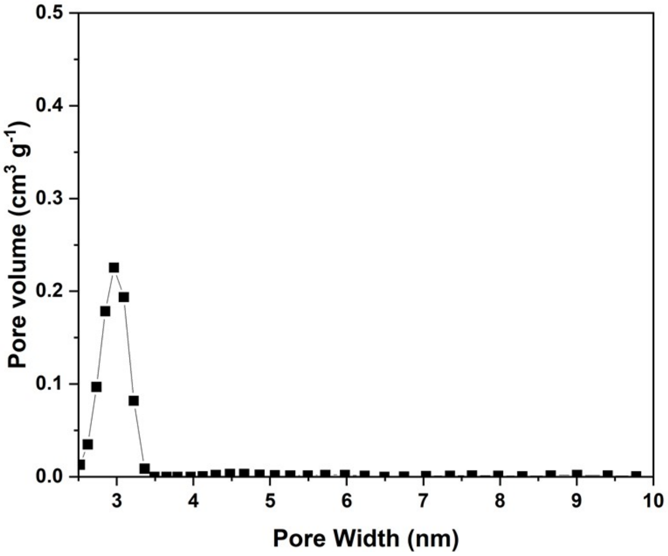

Figure S35. Calculated pore size distribution of COF-S_2C_2-R.

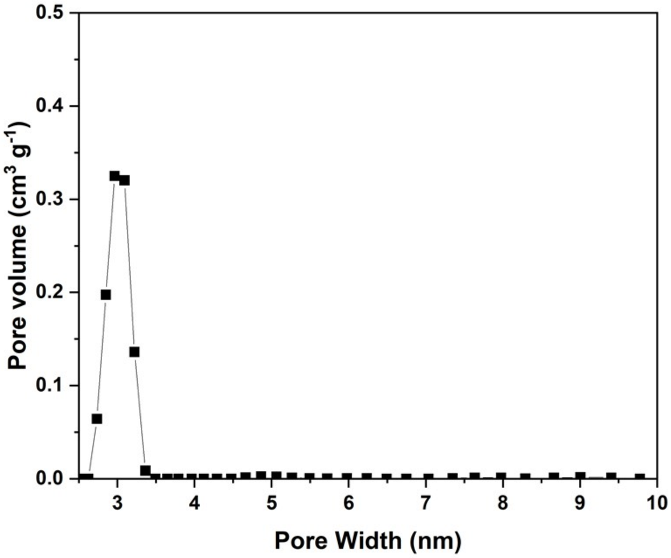

Figure S36. Calculated pore size distribution of COF-S_2C_3-R.

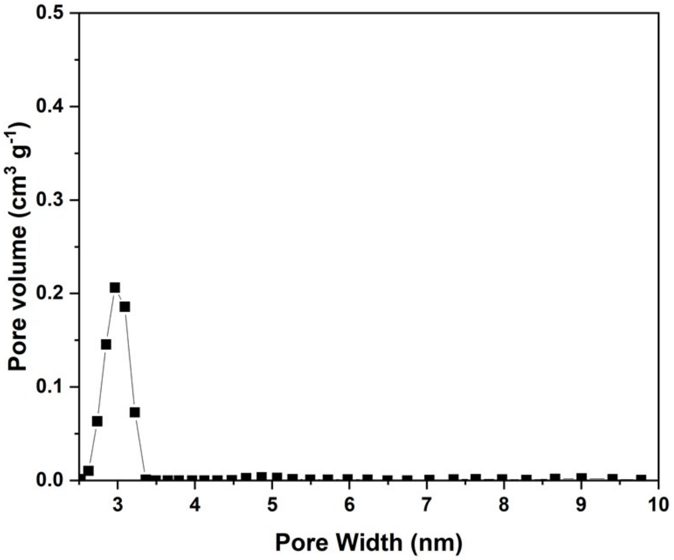

Figure S37. Calculated pore size distribution of COF-S_2C_4-R.

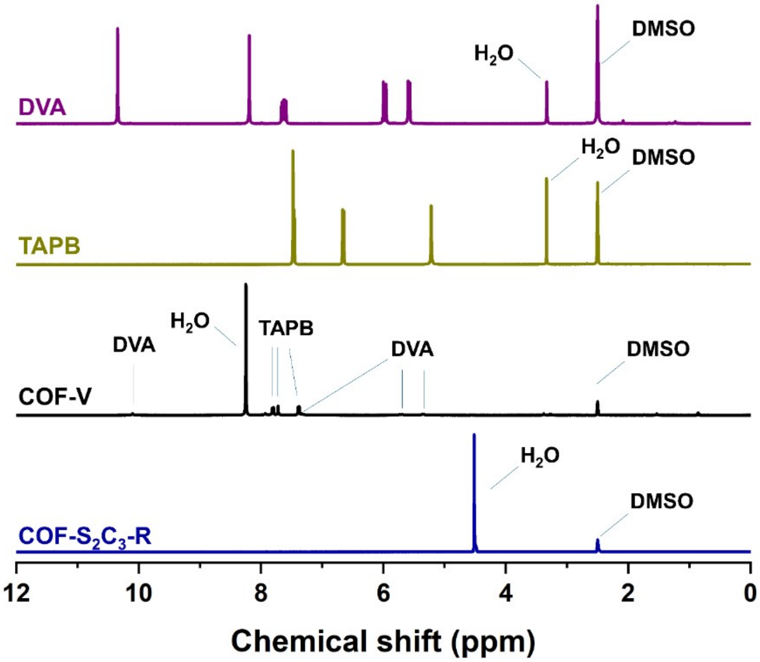

Figure S38. ^{1}H NMR spectrum of COF-V (black) and COF-S_2C_3-R (blue) after DCl:D_2O treatment compared to DVA (purple) and TAPB (gold).

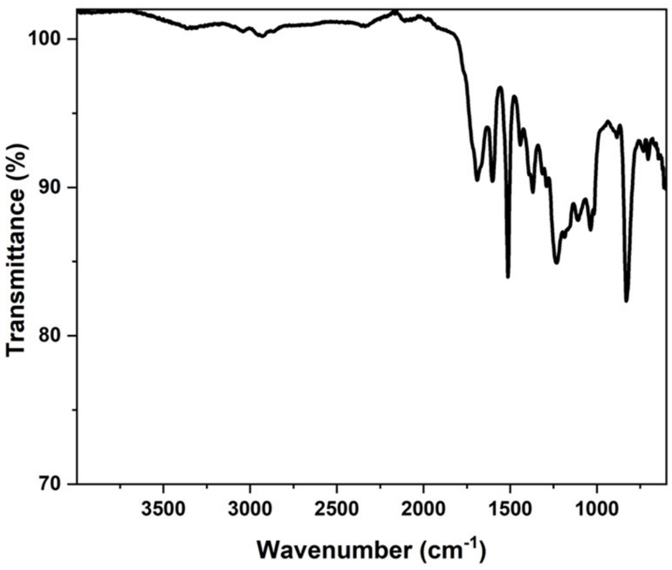

Figure S39. FTIR spectrum of COF-S_2C_3-Ac.

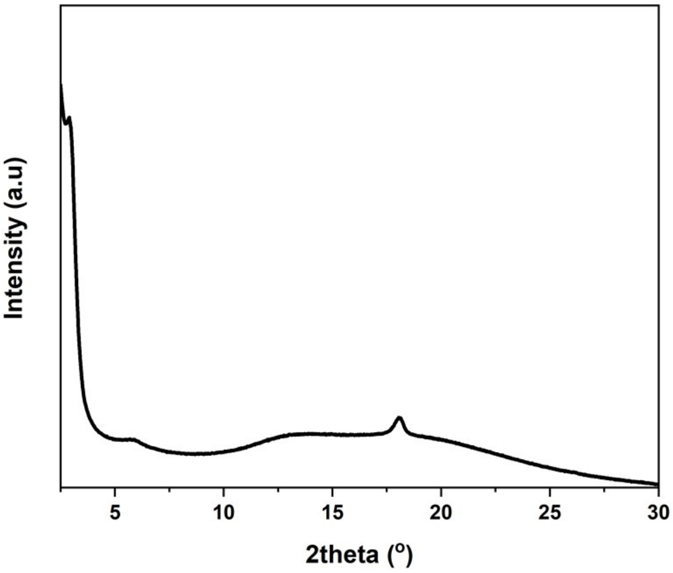

Figure S40. PXRD pattern of COF-S_2C_3-Ac.

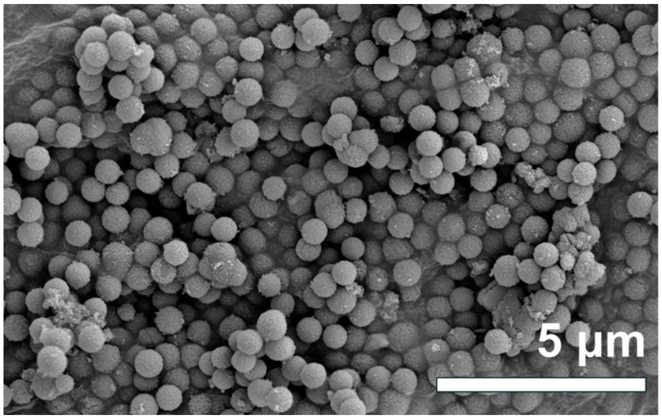

Figure S41. SEM of COF-S_2C_3-Ac

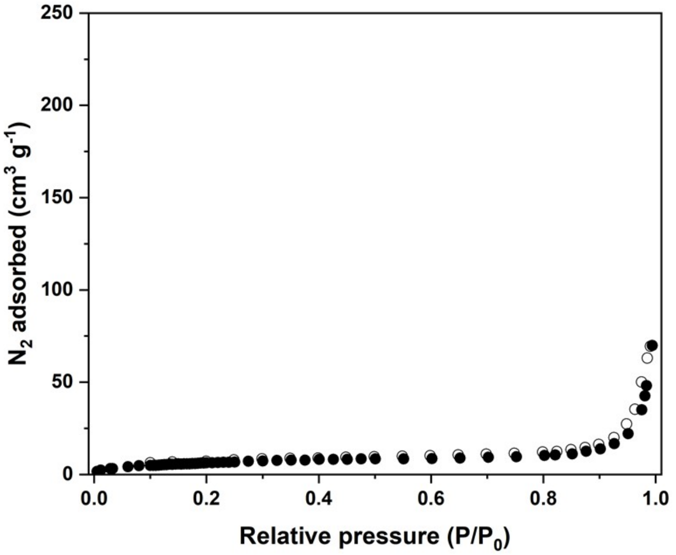

Figure S42. N_2 sorption isotherm of COF-S_2C_3-Ac at 77 K.

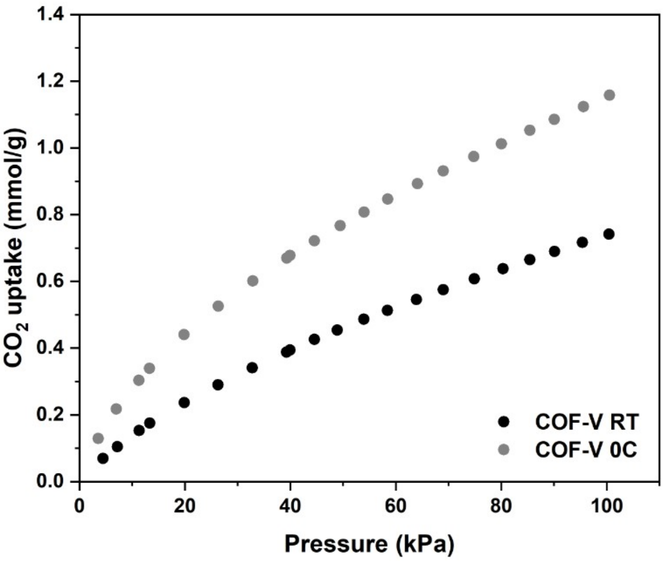

Figure S43. CO_2 adsorption isotherm of COF-V at room temperature (black) and 0 ℃ (grey).

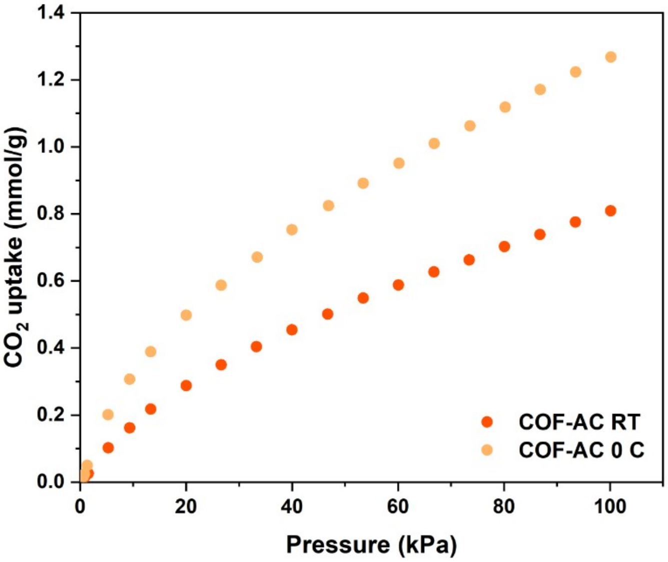

Figure S44. CO_2 adsorption isotherm of COF-S_2C_3-Ac at room temperature (red) and 0 ℃ (orange).

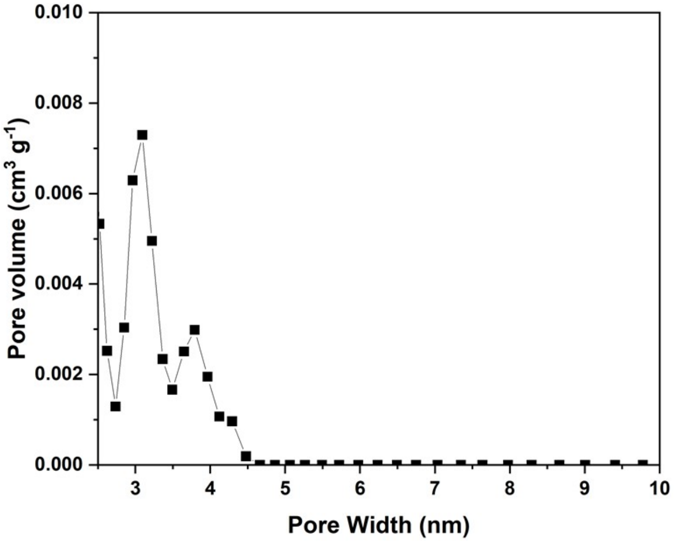

Figure S45. Calculated pore size distribution of COF-S_2C_3-Ac.

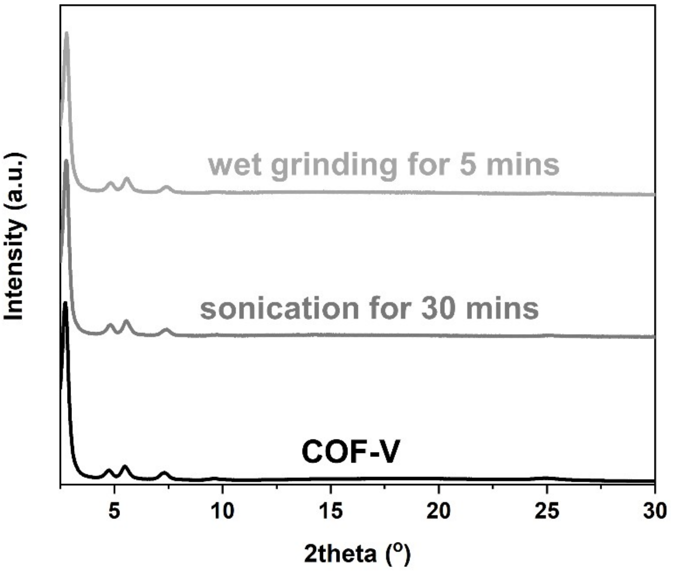

Figure S46. PXRD pattern of COF-V (black) before and after sonication (grey) or grinding (light grey).

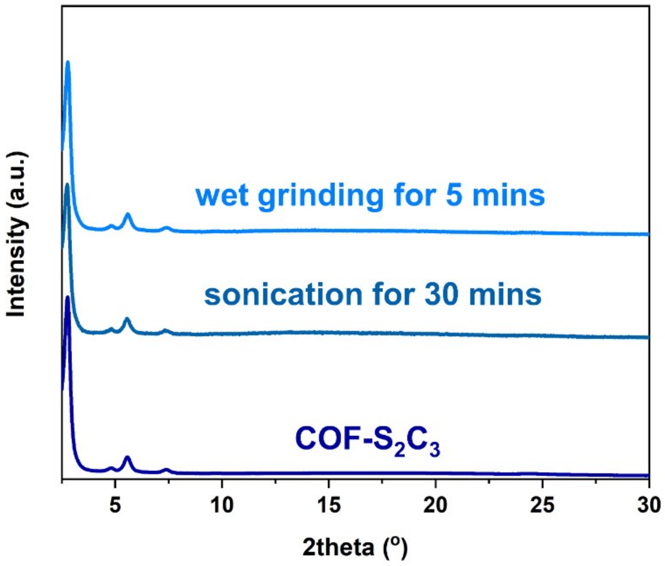

Figure S47. PXRD pattern of COF-S$_2$C$_3$ (dark blue) before and after sonication (blue) or grinding (light blue).

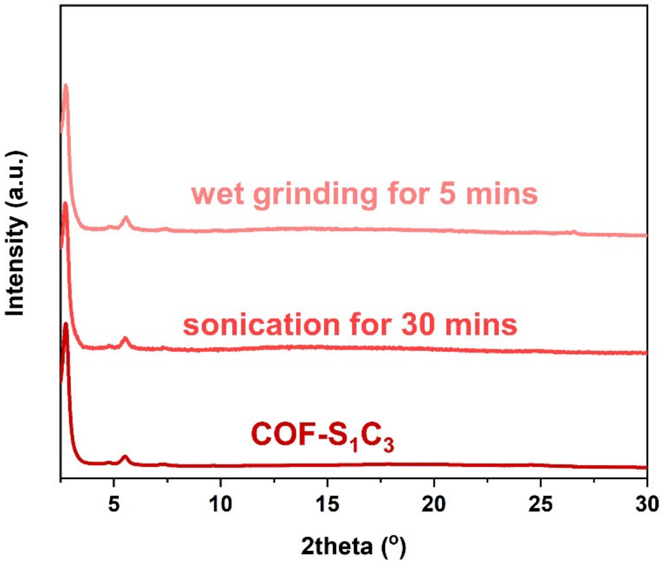

Figure S48. PXRD pattern of COF-S$_1$C$_3$ (dark red) before and after sonication (red) or grinding (light red).

Table S1. Atomistic coordinates for the AA-stacking mode of COF-V optimized geometry using Forcite method (space group P6, a=b=37.7236 Å; c=3.6234 Å, α=β=90° and γ=120°).

Atom	***x/a***	***y/b***	***z/c***
C1	0.553351	0.030205	0.569438
C2	0.540842	-0.00237	0.514235
C3	0.532274	0.06328	0.570172
C4	0.550252	0.095273	0.63032
C5	0.53193	0.127488	0.634357
C6	0.49503	0.12823	0.575393
C7	0.47702	0.096227	0.520139
C8	0.495327	0.064008	0.51588
N9	0.474687	0.160479	0.579765
C10	0.487029	0.192578	0.554612
C11	0.462657	0.223466	0.566805
C12	0.426282	0.218519	0.594237
C13	0.474287	0.258581	0.551396
H14	0.513252	-0.00814	0.46261
H15	0.57864	0.095313	0.676172
H16	0.546793	0.151381	0.689548
H17	0.448589	0.096306	0.478399
H18	0.480299	0.040029	0.470737
H19	0.515007	0.196845	0.515877
H20	0.414284	0.192487	0.607711
C21	0.509244	0.270157	0.527863
H22	0.531304	0.251938	0.521436
C23	0.516483	0.306098	0.513584
H24	0.49535	0.325539	0.519749
H25	0.543646	0.315161	0.495902

Table S2. Experimentally measured C/H/N/S values from combustion analysis of COF-S_2C_2, COF-S_2C_3, COF-S_2C_4, and COF-S_1C_3.

Experimental	**C (%)**	**H (%)**	**N (%)**	**S (%)**
COF-S_2C_2	71.6	4.47	5.84	3.08
COF-S_2C_3	71.1	5.08	5.62	5.72
COF-S_2C_4	68.3	4.80	5.34	4.25
COF-S_1C_3	66.4	5.06	4.97	4.59

Table S3. Calculated C/H/N/S values for COF-S_2C_2, COF-S_2C_3, COF-S_2C_4, and COF-S_1C_3.

Calculated	**C (%)**	**H (%)**	**N (%)**	**S (%)**
COF-S_2C_2	75.28	5.48	5.85	13.40
COF-S_2C_3	75.67	5.81	5.63	12.89
COF-S_2C_4	75.94	6.04	5.48	12.54
COF-S_1C_3	75.64	6.41	5.46	12.49

References

(1) N. Prusinowska, M. Bardziński, A. Janiak, P. Skowronek, M. Kwit, *Chem. Asian J.,* 2018, **13**, 2691–2699.

(2) K. Yoshida, H. Takahashi, T. Imamoto, *Chem. Eur. J.,* 2008, **14**, 8246–8261.

(3) W. P. Gallagher, A. Vo, *Org. Process Res. Dev.,* 2015, **19**, 1369–1373.

(4) J.-T. Ou, M. K. Taylor, *Chem. Commun.,* 2025, **6**, 11420-11426.

(5) W. Ma, Q. Zheng, Y. He, G. Li, W. Guo, Z. Lin, L. Zhang, *J. Am. Chem. Soc.,* 2019, **141**, 18271–18277.

(6) Q. Sun, B. Aguila, J. Perman, L. D. Earl, C. W. Abney, Y. Cheng, H. Wei, N. Nguyen, L. Wojtas, S. Ma, *J. Am. Chem. Soc.,* 2017, **139**, 2786–2793.

(7) S. J. Lyle, T. M. Osborn Popp, P. J. Waller, X. Pei, J. A. Reimer, O. M. Yaghi, *J. Am. Chem. Soc.,* 2019, **141**, 11253–11258.